Published for SISSA by Springer

Received: August 26, 2021
Revised: March 8, 2022
Accepted: March 14, 2022
Published: March 28, 2022

Revisiting type-II see-saw: present limits and future prospects at LHC

Saiyad Ashanujjaman[1] **and Kirtiman Ghosh**

Institute of Physics, Bhubaneswar,
Sachivalaya Marg, Sainik School Post, Bhubaneswar 751005, India
Homi Bhabha National Institute,
Training School Complex, Anushakti Nagar, Mumbai 400094, India

E-mail: saiyad.a@iopb.res.in, kirti.gh@gmail.com

Abstract: The type-II see-saw mechanism based on the annexation of the Standard Model by weak gauge triplet scalar field proffers a natural explanation for the very minuteness of neutrino masses. Noting that the phenomenology for the non-degenerate triplet Higgs spectrum is substantially contrasting than that for the degenerate one, we perform a comprehensive study for an extensive model parameter space parametrised by the triplet scalar vacuum expectation value (VEV), the mass-splitting between the triplet-like doubly and singly charged scalars and the mass of the doubly charged scalar. Considering all Drell-Yan production mechanisms for the triplet-like scalars and taking into account the all-encompassing complexity of their decays, we derive the most stringent 95% CL lower limits on the mass of the doubly charged scalar for a vast model parameter space by implementing already existing direct collider searches by CMS and ATLAS. These estimated limits are stronger by approximately 50–230 GeV than those reported by CMS and ATLAS. Strikingly, we also find a specific region of the parameter space that is beyond the reach of the existing LHC search strategies. Then, we forecast future limits by extending an ATLAS search at high-luminosity, and we propose a search strategy that yields improved limits for a part of the parameter space.

Keywords: Beyond Standard Model, Neutrino Physics

ArXiv ePrint: 2108.10952

[1] https://orcid.org/0000-0001-5643-2652.

https://doi.org/10.1007/JHEP03(2022)195

JHEP03(2022)195

Contents

1 Introduction

The Standard Model (SM) falls short of offering explanations of tiny neutrino masses and mixings. Although plausible, it seems philosophically displeasing that the tiny neutrino masses are effectuated via the usual Brout-Englert-Higgs mechanism as it entails extremely small Yukawa couplings causing hierarchy among them. Conversely, the widely-studied see-saw mechanisms seem to proffer a natural explanation for the very minuteness of neutrino masses. The type-II see-saw model based on the annexation of the SM by weak gauge triplet of scalar field [1–6] is one such variant. Yukawa interaction of the scalar triplet with the SM lepton doublet leads to neutrino masses after its neutral component procure a non-zero vacuum expectation value (VEV). The Yukawa coupling driving the leptonic decays of the non-standard scalars in the model pans out to be determined by the neutrino oscillation parameters up to the triplet VEV (v_t). Though *ad hoc*, this prognostic characteristic of the present scenario makes the same an appealing one beyond the SM (BSM). Not only this model holds out a riveting rationale for the neutrino masses, but it also put forward an elaborated electroweak symmetry breaking (EWSB) mechanism and rich phenomenology at the Large Hadron Collider (LHC). This model contains several triplet-like physical Higgs states, namely doubly charged scalars ($H^{\pm\pm}$), singly charged scalars ($H^{\pm}$) and CP-even and CP-odd neutral scalars (H^0 and A^0). Phenomenological outcome of this model has been studied all-encompassingly in the literature. The main dynamical features of the Higgs potential have been discussed in detail in refs. [7–11]. The Yukawa interaction of the scalar triplet with the SM lepton doublet leads to charged lepton flavour violating decays. This has been addressed in detail in refs. [12–17]. Refs. [18–22] have investigated

JHEP03(2022)195

the possibility to resolve the neutrino mass spectrum and determine the hitherto unknown neutrino oscillation parameters at LHC. Copious production of the triplet-like scalars and their decays to the SM particles caters promising direct ways to probe this model at the LHC. Refs. [23–37] have studied the LHC phenomenology assuming degenerate spectrum for the triplet-like scalars. Refs. [38–40] have pointed out that the pheneomenology for the non-degenerate scenario is substantially contrasting than that for the degenerate one. Phenomenology the non-degenerate scenario also has been studied in refs. [41–50]. Refs. [51, 52] have discussed the possibility of the triplet-like scalars being long-lived, and thus leading to displaced vertex signatures at colliders. A more comprehensive review can be found in refs. [53, 54].

A wealth of BSM models such as the present model [1–6], left-right symmetric models [55–57] Higgs triplet models [58, 59], little Higgs model [60–62], Georgi-Machacek model [63, 64], Zee-Babu model [65, 66] and other extensions of SM [67–72] envisage presence of doubly charged scalar bosons and their illustrious signatures. This is why, a number of searches have been carried out at the LHC by CMS and ATLAS [73–82]. In view of the observations being consistent with the SM background expectations, these searches derived stringent limits with 95% confidence level (CL) on the doubly charged scalar mass. Collider phenomenology of this model, by and large, is governed by three parameters only — $m_{H^{\pm\pm}}$, $\Delta m = m_{H^{\pm\pm}} - m_{H^{\pm}}$ and v_t (see section 2). For degenerate scenario ($\Delta m = 0$), $H^{\pm\pm}$ decays to same-sign dilepton for $v_t < 10^{-4}\,\text{GeV}$ and to same-sign W-boson for $v_t > 10^{-4}\,\text{GeV}$. For $H^{\pm\pm}$ decaying 100% into same-sign dilepton, a search in three and four lepton final states with an integrated luminosity of $12.9\,\text{fb}^{-1}$ of pp collisions at $\sqrt{s} = 13\,\text{TeV}$ LHC by the CMS collaboration [78] has excluded them with mass below 716–761 GeV considering four benchmark points targeting four possible neutrino mass hypotheses. In addition, considering 100% decay of $H^{\pm\pm}$ into lepton (e, μ, τ) pair, the same search has set a limit of 535–820 GeV. Another search in multilepton final states with an integrated luminosity of $36.1\,\text{fb}^{-1}$ of pp collisions at $\sqrt{s} = 13\,\text{TeV}$ LHC by the ATLAS collaboration [79] has set a limit of 770–870 GeV and 450 GeV for $H^{\pm\pm}$ decaying, respectively, 100% and 10% into same-sign light lepton (e, μ) pair. A recent search in multilepton final states, optimised for $H^{\pm\pm}$ decaying exclusively into same-sign W-boson pair, with an integrated luminosity of $139\,\text{fb}^{-1}$ of pp collisions at $\sqrt{s} = 13\,\text{TeV}$ LHC by the ATLAS collaboration [82] has excluded them with masses up to 350 GeV and 230 GeV, respectively, for the pair and associated production modes assuming $v_t = 0.1\,\text{GeV}$ and the mixing between the CP-even scalars to be 10^{-4}.

Evidently, the above-cited limits are not befitting to the entire parameter space, rather valid only for a constrained parameter space of the model. For instance, the CMS search in ref. [78] is only valid for $\Delta m = 0$ and $v_t < 10^{-4}\,\text{GeV}$, whereas the ATLAS search in ref. [82] is only valid for $\Delta m = 0$ and $v_t > 10^{-4}\,\text{GeV}$. Though in a realistic type-II see-saw scenario, the branching fractions of the triplet-like scalars into different lepton flavours are dictated by the neutrino oscillation parameters, most of the aforecited limits are derived in the context of simplified scenarios without reckoning the footprints of the low-energy neutrino parameters. Furthermore, these limits are often conservative as these searches do not incorporate all the Drell-Yan production channels for the triplet-like scalars. However,

JHEP03(2022)195

all the Drell-Yan processes are of sizeable cross-sections, and thus, all of them entail to be incorporated into the analyses. Moreover, the triplet components in this model are conceivably non-degenerate in mass. For moderate v_t and passably large Δm, cascade decays quickly dominate over the leptonic and diboson decay modes, see section 3. Not only does the mass-splitting overwhelm the decays of the triplet-like scalars, but it also affects their production cross-sections at the LHC. Thus, the pheneomenology for the non-degenerate scenario substantially is contrasting than that for the degenerate one [39–42, 45, 46]. Bearing the aforesaid discussion in mind, we perform a systematic and comprehensive collider study of this model. Incorporating all the Drell-Yan production modes for the triplet-like scalars and taking into account the all-encompassing complexity of their decays, we derive the most stringent 95% CL lower limit on $m_{H^{\pm\pm}}$ for a wide range of v_t and Δm by implementing already existing direct collider searches by CMS and ATLAS. Then, we forecast future limits on $m_{H^{\pm\pm}}$ by extending the ATLAS search at high-luminsity, and we propose a search strategy that yields improved limits on $m_{H^{\pm\pm}}$ for a part of the parameter space of v_t and Δm.

The rest of this work is structured as follows. In section 2, we briefly describe the theoretical structure of the type-II see-saw model. Production of the triplet-like scalars and their decays are discussed in section 3. In section 4, we discuss the LHC phenomenology of this model and obtain stringent limits on $m_{H^{\pm\pm}}$ for a wide region of model parameter space.

2 The type-II see-saw model

The scalar sector of the minimal type-II see-saw model employs a $\mathrm{SU}(2)_L$ triplet scalar field with hypercharge 1, Δ in addition to the SM Higgs doublet, Φ:

$$\Delta = \begin{pmatrix} \Delta^+/\sqrt{2} & \Delta^{++} \\ \Delta^0 & -\Delta^+/\sqrt{2} \end{pmatrix} \quad \text{and} \quad \Phi = \begin{pmatrix} \Phi^+ \\ \Phi^0 \end{pmatrix}.$$

The most general renormalizable gauge invariant scalar potential invloving Φ and Δ is given by [7]

$$\begin{aligned} V(\Phi,\Delta) = &-m_\Phi^2 \Phi^\dagger\Phi + \frac{\lambda}{4}(\Phi^\dagger\Phi)^2 + m_\Delta^2 \mathrm{Tr}(\Delta^\dagger\Delta) + [\mu(\Phi^T i\sigma^2 \Delta^\dagger \Phi) + \mathrm{h.c.}] \\ &+\lambda_1(\Phi^\dagger\Phi)\mathrm{Tr}(\Delta^\dagger\Delta) + \lambda_2[\mathrm{Tr}(\Delta^\dagger\Delta)]^2 + \lambda_3 \mathrm{Tr}[(\Delta^\dagger\Delta)^2] + \lambda_4 \Phi^\dagger \Delta\Delta^\dagger\Phi, \end{aligned}$$

where m_Φ^2, m_Δ^2 and μ are the mass parameters, λ and λ_i $(i = 1, \ldots, 4)$ are the independent dimensionless couplings. The neutral components of Φ and Δ can be parametrised as $\Phi^0 = \frac{1}{\sqrt{2}}(v_d + h + iZ_1)$ and $\Delta^0 = \frac{1}{\sqrt{2}}(v_t + \xi + iZ_2)$, where v_d and v_t are their respective VEVs with $\sqrt{v_d^2 + 2v_t^2} = 246\,\mathrm{GeV}$. The degrees of freedom carrying identical electric charges mix after the EWSB,. The neutral states Φ^0 and Δ^0 mix into two CP-even states h^0 and H^0, and two CP-odd states G^0 and A^0, whereas the singly charged states $\Phi^\pm$ and $\Delta^\pm$ mix into mass states $G^\pm$ and $A^\pm$. The doubly charged gauge state $\Delta^{\pm\pm}$ is aligned with its mass state $H^{\pm\pm}$. Therefore, the mixings result into several massive physical states (h^0, H^0, A^0, $H^\pm$ and $H^{\pm\pm}$) and Nambu-Goldstone bosons (G^0 and $G^\pm$) eaten by the longitudinal

JHEP03(2022)195

modes of Z and $W^{\pm}$. The mixing angles in the CP-even, CP-odd and singly-charged Higgs sectors (denoted by α, β_0 and $\beta_{\pm}$, respectively) are given by [7]

$$\tan 2\alpha = \frac{-2\sqrt{2}\mu v_d + 2(\lambda_1+\lambda_4)v_d v_t}{\frac{\lambda}{2}v_d^2 - \frac{\mu v_d^2}{\sqrt{2}v_t} - 2(\lambda_2+\lambda_3)v_t^2} \quad \text{and} \quad \tan\beta_0 = \sqrt{2}\tan\beta_{\pm} = \frac{2v_t}{v_d}.$$

For $v_t \gg v_d$, the CP-even Higgs mixing angle and masses of the physical states reduces to

$$\tan 2\alpha \approx \frac{4v_t}{v_d}\left(1 - \frac{m_{h^0}^2}{m_{H^0}^2}\right)^{-1} \tag{2.1}$$

$$m_{H^{\pm\pm}}^2 \simeq m_\Delta^2 - \frac{\lambda_4}{2}v_d^2, \quad m_{H^{\pm}}^2 \simeq m_\Delta^2 - \frac{\lambda_4}{4}v_d^2, \quad m_{h^0}^2 \simeq 2v_d^2\lambda \quad \text{and} \quad m_{H^0}^2 \approx m_{A^0}^2 \simeq m_\Delta^2,$$

and their mass-squared differences[1] are given by

$$m_{H^{\pm\pm}}^2 - m_{H^{\pm}}^2 \approx m_{H^{\pm}}^2 - m_{H^0/A^0}^2 \approx -\frac{\lambda_4}{4}v_d^2.$$

For usefulness, we define the mass-splitting between $H^{\pm\pm}$ and $H^{\pm}$ as $\Delta m = m_{H^{\pm\pm}} - m_{H^{\pm}}$. Thereby, the masses of all the physical Higgs states can be traded in terms of just two parameters—$m_{H^{\pm\pm}}$ and Δm. The value (sign) of λ_4, thus Δm predicts three characteristic mass spectra: (*i*) $m_{H^{\pm\pm}} \simeq m_{H^{\pm}} \simeq m_{H^0/A^0}$, (*ii*) $m_{H^{\pm\pm}} > m_{H^{\pm}} > m_{H^0/A^0}$ and (*iii*) $m_{H^{\pm\pm}} < m_{H^{\pm}} < m_{H^0/A^0}$. We refer to these mass spectra as degenerate, positive and negative scenario, respectively.

The Yukawa interaction of the scalar triplet with the SM lepton doublet $L = (\nu_L, \ell_L)^T$ is given by

$$-\mathcal{L}_\nu = Y_{ij}^\nu L_i^T C i\sigma^2 \Delta L_j + \text{h.c.},$$

where Y^ν is a 3×3 symmetric complex matrix, i and j are the generation indices ($i,j = 1,2,3$), and C is the charge-conjugation matrix. This interaction leads to majorana masses for the neutrinos after the EWSB:

$$m_\nu = \sqrt{2}Y^\nu v_t. \tag{2.2}$$

m_ν can be diagonalised using the Pontecorvo-Maki-Nakagawa-Sakata matrix U which is parametrised by three mixing angles, one dirac phase and two Majorana phases: $U^T m_\nu U = \text{diag}(m_1, m_2, m_3)$. For simplicity, we set the phases to zero as they are either poorly measured or hitherto not measured. Measurements of large scale structure in the universe by the Planck satellite has put a bound $\sum_i m_i < 0.12\,\text{eV}$ when combined with baryon acoustic oscillation data [84]. The best fit values for the neutrino oscillation parameters used in this work are taken from ref. [85].

[1] In addition to the tree-level mass-splitting, radiative corrections dominantly driven by the electroweak gauge bosons induce mass-splittings among different triplet scalars: $m_{H^{\pm\pm}} - m_{H^{\pm}} \sim 885\,\text{MeV}$ and $m_{H^{\pm}} - m_{H^0/A^0} \sim 540\,\text{MeV}$ [83]. These mass-splittings exclusively are not large enough to have considerable effects on their decays and thereby neglected [22].

JHEP03(2022)195

Phenomenologically relevant parameters. While the Yukawa couplings are determined by the neutrino oscillation parameters[2] up to v_t (see eq. 2.2), all the scalar potential parameters can be framed in terms of the physical Higgs masses, v_t and α [7]. The mixing angle is further determined in terms of the others (see eq. 2.1). Moreover, the masses can be traded in terms of just two parameters—$m_{H^{\pm\pm}}$ and Δm. Therefore, the phenomenology of this model, by and large, is governed by three parameters only—$m_{H^{\pm\pm}}$, Δm and v_t. Before concluding this section, we briefly discuss the relevant constraints on these parameters:

(*i*) The value of the ρ parameter from the electroweak precision data, $\rho = 1.00038(20)$ [86], which is 1.9σ above the SM expectation at tree level leads to an upper bound of $\mathcal{O}(1)$ GeV on v_t ($\ll v_d$).

(*ii*) The electroweak precision data observables, namely S, T and U parameters tightly constrain the mass-splittings requiring $|\Delta m| \lesssim 40$ GeV [9, 11, 49, 87].

(*iii*) The SM Higgs-to-diphoton decay rate at the LHC requires $|\sin\alpha| \lesssim 0.3$ at 95% CL [49].

(*iv*) The Yukawa interaction leads to lepton flavour violating decays such as $\ell_\alpha \to \ell_\beta\gamma$ at 1-loop and $\ell_\alpha \to \ell_\beta\ell_\gamma\ell_\delta$ at tree level. The upper limits on the branching fractions of $\mu^- \to e^-\gamma$ [88] and $\mu^- \to e^+e^-e^-$ [89] robustly constrain the v_t–$m_{H^{\pm\pm}}$ parameter space [13–15]:

$$v_t \gtrsim 0.78\text{–}1.5(0.69\text{–}2.3) \times 10^{-9}\ \text{GeV} \times \frac{1\,\text{TeV}}{m_{H^{\pm\pm}}}$$

for normal (inverted) hierarchical neutrino mass spectrum consistent with the bound from cosmology [85].

3 Production and decays of triplet scalars

The TeV scale triplet-like scalars are pair produced copiously at the LHC by quark-antiquark annihilation via the neutral current and charged current Drell-Yan mechanisms:[3]

$$q\bar{q}' \to W^* \to H^{\pm\pm}H^{\mp}, H^{\pm}H^0, H^{\pm}A^0 \quad \text{and} \quad q\bar{q} \to \gamma^*/Z^* \to H^{\pm\pm}H^{\mp\mp}, H^{\pm}H^{\mp}, H^0A^0.$$

We implement the model in `SARAH` [94, 95] to generate `UFO` modules, and use `MadGraph` [96, 97] with the `NNPDF23_lo_as_0130_qed` parton distribution function [98, 99] for numerical evaluation of the leading order (LO) production cross-sections of the triplet

[2] Some of the neutrino oscillation parameters, namely the lightest neutrino mass and the CP phases, are either poorly measured or hitherto not measured. In this work, we set the phases to be zero for simplicity. However, note that these parameters could substantially change the leptonic decays and thereby the phenomenology of the triplet-like scalars [22, 37].

[3] Also, the triplet-like scalars are produced via t/u-channel photon fusion [90, 91] and vector boson-fusion processes [23, 92, 93], with two associated forward jets at the LHC. However, their production through such processes is sub-dominant for the mass range of our interest, and thus neglected. That said, the photon fusion process become important for large masses of the triplet scalars, and thus, entail to be incorporated into the analyses for multi-TeV scalar masses at high-energy LHC.

JHEP03(2022)195

scalars at the 13 TeV LHC. All the Drell-Yan production mechanisms are of sizeable cross-sections [27–37, 40–50]. In particular, production of the doubly charged scalars in association with the singly charged ones, which is sometimes precluded by experimental searches, has the largest cross-section for both degenerate and negative scenarios. Production of the singly charged scalars in association with the neutral ones, which is also forsaken by both CMS and ATLAS, has the largest cross-section for both degenerate and positive scenarios. This substantiates that all the channels entail to be incorporated into the analyses.

Refs. [25, 100] have estimated the QCD corrections to the production of doubly charged scalars at hadron colliders which result in a next-to-leading (NLO) K-factor of 1.2–1.3. Considering that the QCD corrections to the production of singly charged scalars are similar to those of doubly charged ones, we apply an overall QCD K-factor of 1.25 to the LO cross-section.

We next discuss the decays of the triplet-like scalars. Their decays have been well studied in the literature [22, 40, 101–104].[4] The doubly charged scalars have three possible decay modes: (*i*) leptonic decay, i.e. $\ell^\pm\ell^\pm$, (*ii*) gauge boson decay, i.e. $W^\pm W^\pm$, and (*iii*) cascade decay, i.e. $H^\pm W^{\pm *}$. The latter decay mode kinematically opens up only for $\Delta m > 0$. For $m^2_{H^{\pm\pm}} \gg m^2_W$, the ratio of the braching fractions for these modes are obtained as

$$\frac{1}{4}\left(\frac{m_\nu}{m_{H^{\pm\pm}}}\right)^2\left(\frac{v_d}{v_t}\right)^2 : \left(\frac{v_t}{v_d}\right)^2 : \frac{12}{5\pi^2}\frac{\max(\Delta m,0)^5}{v_d^2 m^3_{H^{\pm\pm}}}.$$

$H^{\pm\pm}$ decays into $\ell^\pm\ell^\pm$ and $W^\pm W^\pm$ for $\Delta m < \mathcal{O}(1)\,\text{GeV}$. These two decay modes are comparable for $v_t \sim \mathcal{O}(10^{-4})\,\text{GeV}$, and the former dominates over the latter for $v_t < 10^{-4}\,\text{GeV}$ and vice versa. The cascade mode starts to contribute for $\Delta m \gtrsim \mathcal{O}(1)\,\text{GeV}$ and become dominant for large Δm.

The singly charged scalars have four decay modes: (*i*) leptonic decay, i.e. $\ell^\pm\nu$, (*ii*) hadronic decay, i.e. $t\bar{b}$, (*iii*) diboson decay, i.e. $W^\pm Z/h^0$, and (*iv*) cascade decay, i.e. $H^0/A^0 W^{\pm *}$ or $H^{\pm\pm}W^{\mp *}$. These cascade modes kinematically open up, respectively, for $\Delta m > 0$ and $\Delta m < 0$. For $m^2_{H^\pm} \gg m^2_W$, the ratio of the braching fractions for $\ell^\pm\nu$, $t\bar{b}$, $W^\pm Z$, $W^\pm h^0$, $H^0/A^0W^{\pm *}$ and $H^{\pm\pm}W^{\mp *}$ decay modes are evaluated as

$$\begin{aligned}\frac{1}{2}\left(\frac{m_\nu}{m_{H^\pm}}\right)^2\left(\frac{v_d}{v_t}\right)^2 : 6\left(\frac{m_t}{m_{H^\pm}}\right)^2\left(\frac{v_t}{v_d}\right)^2 : \left(\frac{v_t}{v_d}\right)^2 : (1-2\zeta)^2\left(\frac{v_t}{v_d}\right)^2 \\ : \frac{12}{5\pi^2}\frac{\max(\Delta m,0)^5}{v_d^2 m^3_{H^\pm}} : \frac{24}{5\pi^2}\frac{\max(0,-\Delta m)^5}{v_d^2 m^3_{H^\pm}}\end{aligned}$$

where $\zeta = \frac{v_d}{2v_t}\sin\alpha$ and m_t is the top quark mass. For $|\Delta m| < \mathcal{O}(1)\,\text{GeV}$, $H^\pm$ decays into $\ell^\pm\nu$, $t\bar{b}$, $W^\pm Z$ and $W^\pm h^0$. The leptonic mode dominates for $v_t < 10^{-4}\,\text{GeV}$, while the hadronic and diboson modes dominate for $v_t > 10^{-4}\,\text{GeV}$. Further, the diboson mode dominates over the hadronic one for $m^2_{H^\pm} > 3m_t^2$ and vice versa. The cascade modes begin to contribute for $|\Delta m| \gtrsim \mathcal{O}(1)\,\text{GeV}$, and quickly dominate for larger $|\Delta m|$.

[4] We find a few typos in some of the decay width expressions in literature. For instance, there is an extra factor of 4 in the denominator in eq. (A2) and an extra factor of π in the denominator in eq. (A15) in ref. [40]. Likewise, there should be another factor of 2 in the denominator in eq. (7) in ref. [39].

JHEP03(2022)195

The CP-odd (CP-even) heavy neutral scalar has four decay modes: (i) leptonic decay, i.e. $\nu\nu$, (ii) hadronic decay, i.e. $q\bar{q}$ with $q \ni b, t$, (iii) diboson decay, i.e. $h^0 Z$ (WW,ZZ,h^0h^0), and (iv) cascade decay, i.e. $H^{\pm}W^{\mp *}$. The latter decay mode kinematically opens up only for $\Delta m < 0$. For $m^2_{H^0} \gg m^2_W$, the ratio of the braching fractions for $\nu\nu$, $q\bar{q}$, h^0h^0, WW, ZZ and $H^{\pm}W^{\mp *}$ decay modes of H^0 can be estimated as

$$\frac{1}{2}\left(\frac{m_\nu}{m_{H^0}}\right)^2\left(\frac{v_d}{v_t}\right)^2 : 12\zeta^2\left(\frac{m_q}{m_{H^0}}\right)^2\left(\frac{v_t}{v_d}\right)^2 : \zeta^2\left(\frac{v_t}{v_d}\right)^2 : 2(1-\zeta)^2\left(\frac{v_t}{v_d}\right)^2 : 4\left(1-\frac{\zeta}{2}\right)^2\left(\frac{v_t}{v_d}\right)^2 : \frac{12}{5\pi^2}\frac{\max(0,-\Delta m)^5}{v_d^2 m^3_{H^0}}.$$

Likewise, the ratio of the braching fractions for $\nu\nu$, $q\bar{q}$, h^0Z and $H^{\pm}W^{\mp *}$ decay modes of A^0 are evaluated as

$$\frac{1}{4}\left(\frac{m_\nu}{m_{A^0}}\right)^2\left(\frac{v_d}{v_t}\right)^2 : 6\left(\frac{m_q}{m_{A^0}}\right)^2\left(\frac{v_t}{v_d}\right)^2 : (1-2\zeta)^2\left(\frac{v_t}{v_d}\right)^2 : \frac{6}{5\pi^2}\frac{\max(0,-\Delta m)^5}{v_d^2 m^3_{A^0}}.$$

For $-\Delta m < \mathcal{O}(1)\,\text{GeV}$, $A^0(H^0)$ decays into neutrinos and hadrons/dibosons, respectively, for $v_t < 10^{-4}\,\text{GeV}$ and $v_t > 10^{-4}\,\text{GeV}$. Further, the diboson mode dominates over the hadronic one for $m^2_{A^0(H^0)} > 6m_t^2$ as well as for $m^2_{A^0(H^0)} < 4m_t^2$. The cascade mode starts to contribute for $-\Delta m \gtrsim \mathcal{O}(1)\,\text{GeV}$, and shortly dominates for larger $-\Delta m$.

4 Collider searches

Profuse Drell-Yan production of the triplet-like scalars and their subsequent prompt decays[5] to SM particles lead to a variety of final state signatures at the LHC. Possible final states include smoking gun signatures like two pairs of same-sign lepton or two pairs of same-sign W-boson. Phenomenological consequence of the present model at the LHC has been studied extensively in the literature [9–48, 48–54, 90, 92, 105–109]. Rightfully, central attention of most of those studies pivots around the doubly charged scalars because of their distinct decay signatures. For the very same reason, both the CMS and ATLAS collaborations have carried out a number of collider searches at the LHC [73–82]. Hitherto no significant excess over the SM background expectations has been observed in any of these direct seraches. These seraches thereupon have set stringent limits with 95% CL on the masses of the doubly charged scalars. As argued in section 1, these limits are not befitting to the entire model parameter space. Also, these limits are often conservative as these searches do not incorporate all Drell-Yan production channels for the triplet-like scalars. Furthermore, most of these limits are derived in the context of simplified scenarios without reckoning the footprints of the low-energy neutrino parameters.

The quartic scalar interaction $\lambda_4\Phi^\dagger\Delta\Delta^\dagger\Phi$ entitles the triplet components to split in mass. For moderate v_t and passably large Δm, cascade decays quickly dominate over the leptonic and diboson modes. Not only does the mass-splitting overwhelm the decays of the triplet-like scalars, but it also affects their production cross-sections at the LHC. Thus, the

[5] For $v_t > 10^{-4}\,\text{GeV}$ and $m_{H^{\pm\pm}} < 2m_W$, $H^{\pm\pm}$ deacys to $W^{\pm}W^{\pm *}$. For a region of v_t–$m_{H^{\pm\pm}}$ parameter space, $H^{\pm\pm}$ could be long-lived and have displaced vertex signatures at collider [51].

JHEP03(2022)195

pheneomenology for the non-degenerate scenario substantially is contrasting than that for the degenerate one [39–42, 45, 46].

We next briefly discuss the possible final state signatures, and outline already existing direct collider searches by CMS and ATLAS which are potentially sensitive in constraining different parts of the model parameter space.

Degenerate scenario. All the Drell-Yan production mechanisms for the triplet-like scalars except H^+H^- are of sizeable cross-sections. For $v_t < \mathcal{O}(10^{-4})$ GeV, $H^{\pm\pm}$, $H^\pm$ and H^0/A^0 decay to $\ell^\pm\ell^\pm$, $\ell^\pm\nu$ and $\nu\nu$, respectively. Production of $H^{\pm\pm}H^\mp$ and $H^{++}H^{--}$ lead to, respectively, three and four light leptons (e, μ) in the final state. Though $H^\pm H^0/A^0$ and H^0A^0 have sizeable cross-sections, they fall through to complement the multilepton final state because of their invisible decays. The already existing multilepton searches by CMS and ATLAS in refs. [78, 79, 110, 111] are expected to constrain this part of the parameter space.

For $v_t > 10^{-4}$ GeV, $H^{\pm\pm}$, $H^\pm$, H^0 and A^0 decay to $W^\pm W^\pm$, $W^\pm Z/h^0$, $ZZ/WW/h^0h^0$ and h^0Z, respectively. All the production channels give rise multiboson leading into multilepton final states. Therefore, one anticipates this part of the parameter space to be probed by the existing multiboson leading into multilepton searches by ATLAS in refs. [81, 82].

Negative scenario. For $\Delta m \lesssim \mathcal{O}(1)$, this scenario resembles the degenerate one. For passably large Δm and moderate v_t, the cascade decays $H^0/A^0 \to H^\pm W^{\mp *}$ and $H^\pm \to H^{\pm\pm}W^{\mp *}$ dominate over the other decays, thereby enhancing the effective production cross-section for $H^{\pm\pm}$. Then, depending on v_t, $H^{\pm\pm}$ decays into $\ell^\pm\ell^\pm$ and/or $W^\pm W^\pm$. Therefore, this scenario can be probed using the multilepton searches in refs. [78, 79, 110, 111] and/or multiboson leading into multilepton searches in refs. [81, 82].

Positive scenario. Again, this scenario resembles the degenerate one for small Δm. For passably large enough Δm and moderate v_t, the cascade decays $H^{\pm\pm} \to H^\pm W^{\pm *}$ and $H^\pm \to H^0/A^0W^{\pm *}$ dominate over the other decays. This enhances the effective production cross-section for H^0 and A^0. For $v_t > 10^{-4}$ GeV, H^0 and A^0 decay to $ZZ/WW/h^0h^0$ and h^0Z, respectively. This gives rise to multiboson final state signatures. Therefore, one expects this part of the parameter space to be probed by the existing ATLAS searches in refs. [81, 82].[6]

For $v_t < 10^{-4}$ GeV, both H^0 and A^0 decay invisibly into neutrinos. The relevant production mechanisms $H^{\pm\pm}H^\mp$ and $H^{++}H^{--}$ yield soft leptons or jets resulting from the off-shell W-bosons and neutrinos. Being very soft, these final state leptons/jets are very difficult to reconstruct at the LHC. Therefore, in this scenario, the most optimistic final states would be an energetic jet resulting from initial state radiation plus large missing

[6]For large enough Δm and $v_t \sim 10^{-3}$–10^{-4} GeV, the existing searches in refs. [81, 82] fall short in probing the triplet-like scalars. In such a scenario, H^0 dominantly decays to h^0h^0 and ZZ, and A^0 decays to h^0Z. The leptonic decays of Z give rise to multilepton final states. However, the Z-veto used to suppress the oversized background from the Drell-Yan processes makes these searches insensitive in probing this scenario. On the contrary, for hadronic decays of h^0 and Z, the signal cross-section is small compared to the overwhelming QCD jets background, and thus probing this scenario is very challenging.

JHEP03(2022)195

transverse momentum [112–114] or two/three soft leptons plus missing transverse momentum [115, 116]. Therefore, the recent monojet search by ATLAS [112] and the soft leptons searches by CMS [115, 116] could be apparently sensitive in probing this scenario.[7]

4.1 Multilepton final states search by CMS [110]

The CMS collaboration has published a multilepton final states search [110] with an integrated luminosity of 137.1 fb^{-1} of pp collisions at $\sqrt{s} = 13\,\text{TeV}$. This search targeted the triplet fermions in the type-III see-saw model [117]. However, because of similar multilepton final state signatures, this search is conjectured to be sensitive in probing the type-II see-saw model. Hitherto, there is no multilepton search targeting the type-II see-saw model using the full Run-2 dataset by CMS or ATLAS. Thereupon, we set forth to implement this search meticulously.

We simulate the signal events using `MadGraph` [96, 97] with the `NNPDF23_lo_as_0130_qed` parton distribution function [98, 99]. The subsequent decays, initial state radiation (ISR), final state radiation (FSR), showering, fragmentation and hadronisation are simulated with `PYTHIA` [118]. Hadronized events are passed into `Delphes` [119] for object reconstruction and selection, defining signal regions and event selection. In doing so, we rigorously follow the search strategy in ref. [110]. Lastly, we use a hypothesis tester which uses a library of `C++` classes `RooFit` [120] in the `ROOT` environment to estimate CL.

The selected events are categorised into several mutually exclusive signal regions (SRs), namely *3LOSSF0, 3LOSSF1, 4LOSSF0, 4LOSSF1* and *4LOSSF2*, based on the multiplicity of light leptons, the multiplicity and mass of opposite-sign same-flavour (OSSF) lepton pairs, N_{OSSF} and M_{OSSF}. The names of the SRs are self-explanatory, see ref. [110] for details. The events in the *3LOSSF1* SR are further classified as *3L below-Z, 3L on-Z* and *3L above-Z* when M_{OSSF} is below, within and above the Z-boson mass window ($M_Z \pm 15$), respectively. All the SRs are further divided into several independent signal bins using a primary kinematic discriminant, thereby resulting in 40 signal bins in total. For *3L on-Z* SR, this search uses transverse mass (M_T),[8] as the primary discriminant, whereas for all other SRs, scalar sum of the transverse momenta of all charged leptons (L_T) plus the missing transverse momentum (p_T^{miss}) is used. These variables, exploiting the relatively high momenta of the decay products, are found to be useful in discriminating the signal from the background. For the detailed description of our implementation of this search [110], see refs. [121, 122]. The implementation of this search has been validated in

[7] It turns out that both the monojet search by ATLAS and soft leptons search by CMS fail to constrain this scenario. Monojet search usually requires a larger signal cross-section to suppress the vast SM background and is thus usually applicable to the strongly produced particles decaying into soft leptons/jets plus missing particles. Furthermore, the soft lepton final states are suppressed by W-leptonic branching fractions. Inconsiderably small signal cross-section compared to the SM background in the present scenario makes the same very challemging to probe.

[8] The transverse mass is defined as $M_T = \sqrt{2p_T^{\text{miss}} p_T^{\ell}[1 - \cos(\Delta\phi_{\vec{p}_T^{\text{miss}}, \vec{p}_T^{\ell}})]}$, where $\vec{p}_T^{\ell}$ is the transverse momentum vector of the lepton which is not a part of the on-Z pair, and $\Delta\phi_{\vec{p}_T^{\text{miss}}, \vec{p}_T^{\ell}}$ is the azimuthal separation between $\vec{p}_T^{\text{miss}}$ and $\vec{p}_T^{\ell}$.

JHEP03(2022)195

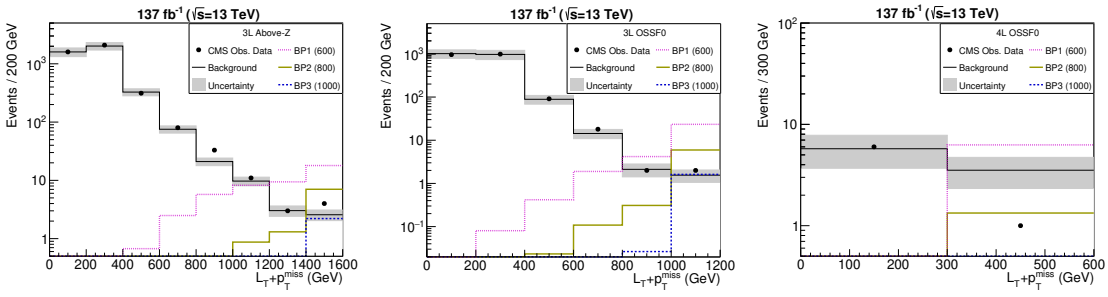

Figure 1. $L_T + p_T^{\text{miss}}$ distributions of the expected background, signal and observed events for *3L above-Z* (left), *3OSSF0* (middle) and *4OSSF0* (right) SRs. The signal predictions are shown for three benchmark masses. See text for details.

previously published work [121] (see figure 10 in ref. [121]). This successful implementation enables us to use the distributions of expected SM backgrounds and observed events in ref. [110] to constrain the type-II see-saw scalars in various v_t–Δm regions. Figure 1 shows the $L_T + p_T^{\text{miss}}$ distributions of the expected SM background events (histograms with black line),[9] the observed events (big black dots) and the expected signal events corresponding to 137.1 fb^{-1} integrated luminosity data at the 13 TeV LHC for three SRs—*3L above-Z* (left), *3OSSF0* (middle) and *4OSSF0* (right). For brevity, we do not show similar distributions for the other SRs. The magenta dotted, dark yellow solid and blue dashed histrograms show the expected signal events for three benchmark masses — 600, 800 and 1000 GeV for $v_t = 10^{-8}$ GeV[10] and $\Delta m = 0$ assuming NH neutrino mass spectrum with $m_1 = 0.03$ eV.[11]

4.2 Multiboson leading to multilepton final states search by ATLAS [82]

The ATLAS collaboration has recently published a search for doubly and singly charged Higgs bosons decaying into vector bosons in multilepton final states with an integrated luminosity of 139 fb^{-1} of pp collisions at $\sqrt{s} = 13$ TeV [82]. As mentioned earlier, this ATLAS search considered either pair or associated production modes for the doubly charged scalars, but not both at once. Also, this search does not incorporate the Drell-Yan production channels for the singly charged and neutral triplet-like scalars. Thus, the limits set by this ATLAS search are conservative. Furthermore, these limits are not befitting to the entire parameter space, rather valid only for $\Delta m = 0$ and $v_t > \mathcal{O}(10^{-4})$ GeV. Therefore, we set forth to recast this search by incorporating all the Drell-Yan production modes for the triplet-like scalars to constrain them for a vast v_t–Δm region. For the implementation, we minutely follow the search strategy in ref. [82].

After object reconstruction and selection (see ref. [82]), the events are categorised into three mutually exclusive analysis channels, namely same-sign dilepton ($2\ell^{sc}$), three

[9] The gray bands represent the total (systematic + statistical) uncertainty on the expected SM background.

[10] The CMS multilepton search in ref. [110] is designed to probe final states with hard-p_T leptons, and hence sensitive to small v_t region where the scalars directly decay to leptons, and results into hard signal leptons in the final state.

[11] For NH, 0.03 eV is the maximum possible value for the lightest neutrino mass consistent with the bound from cosmology.

JHEP03(2022)195

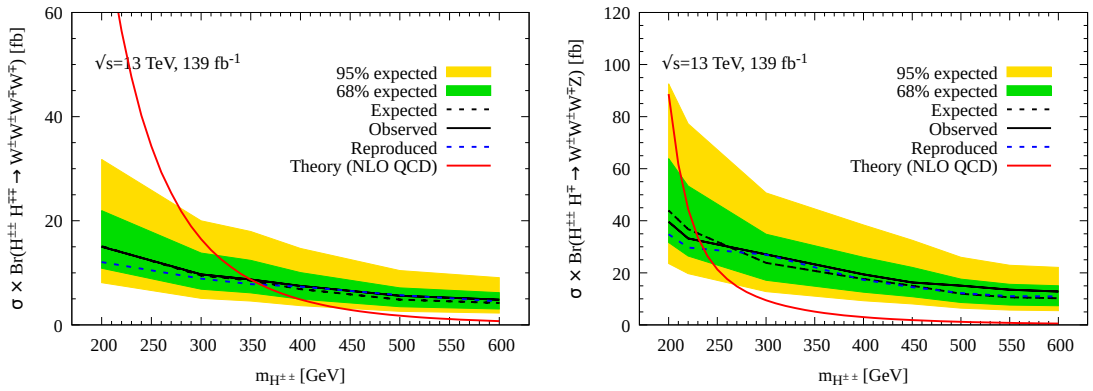

Figure 2. Left (right): the ATLAS observed and expected 95% CL upper limits on the $H^{\pm\pm}H^{\pm\pm}$ ($H^{\pm\pm}H^{\mp}$) production cross-section times branching fraction. The reproduced 95% CL upper limit is represented by the blue dashed curve.

leptons (3ℓ) and four leptons (4ℓ) channels. The event selection proceeds in two steps — the preselection and the SRs selection. The preselection requirements are based on a number of variables such as the absolute value of the sum of charges of the leptons, their transverse momenta, p_T^{miss}, the jet multiplicity, the b-jet multiplicity, M_{OSSF}, etc. Four signal regions (*SR1, SR2, SR3* and *SR4*) are defined for each channel. For defining SRs, several other variables such as the invariant mass of all selected leptons, the invariant mass of all the jets, the distance between two same-sign leptons in the η-ϕ plane, the azimuthal distance between the dilepton system and p_T^{miss}, the smallest distance between any lepton and its closest jet in the η-ϕ plane, etc. are used (see ref. [82] for details).[12] These variables, exploiting the boosted decay topology of the triplet-like Higgs bosons as well as the high energy of their decay products, are useful to discriminate between the signal and the background. Events in the $2\ell^{sc}$ SRs are further divided into $ee, \mu\mu$ and $e\mu$ final states, whereas those in the 3ℓ SRs are separated into two categories ($3\ell1$ and $3\ell0$) based on whether or not an OSSF lepton pair exists in the event. This enhances the sensitivity of this search by distinguishing the lepton-flavour composition between signal and background.

We, then, move forward to validate our implementation of this search by reproducing the ATLAS 95% CL bound on the total pair production cross-section times branching fraction for two scenarios corresponding to the pair production $H^{\pm\pm}H^{\pm\pm}$ and the associated production $H^{\pm\pm}H^{\mp}$ in ref. [82]. The left (right) plot in figure 2 shows the ATLAS observed and expected 95% CL upper limits on the $H^{\pm\pm}H^{\pm\pm}$ ($H^{\pm\pm}H^{\mp}$) production cross-section

[12]Though different sets of kinematic variables and selection cuts are used to define the SRs (*SR1, SR2, SR3* and *SR4*), they are not mutually exclusive. They are designed by optimising the sensitivity for the $H^{\pm\pm}$ pair production mode, respectively, for the $m_{H^{\pm\pm}} = 200$, 300, 400 and 500 GeV mass hypotheses. ref. [82] considers *SR1*(*SR2*){*SR3*}[*SR4*] for 200–300(300–400){400-500}[$>$ 500] GeV mass hypothesis. Here, we differ from ref. [82]; for a given mass hypothesis, we conider all the SRs disjointly, and eventually, choose the most sensitive one. However, for the validation of our implementation, we adhere to the ref. [82]'s approach.

JHEP03(2022)195

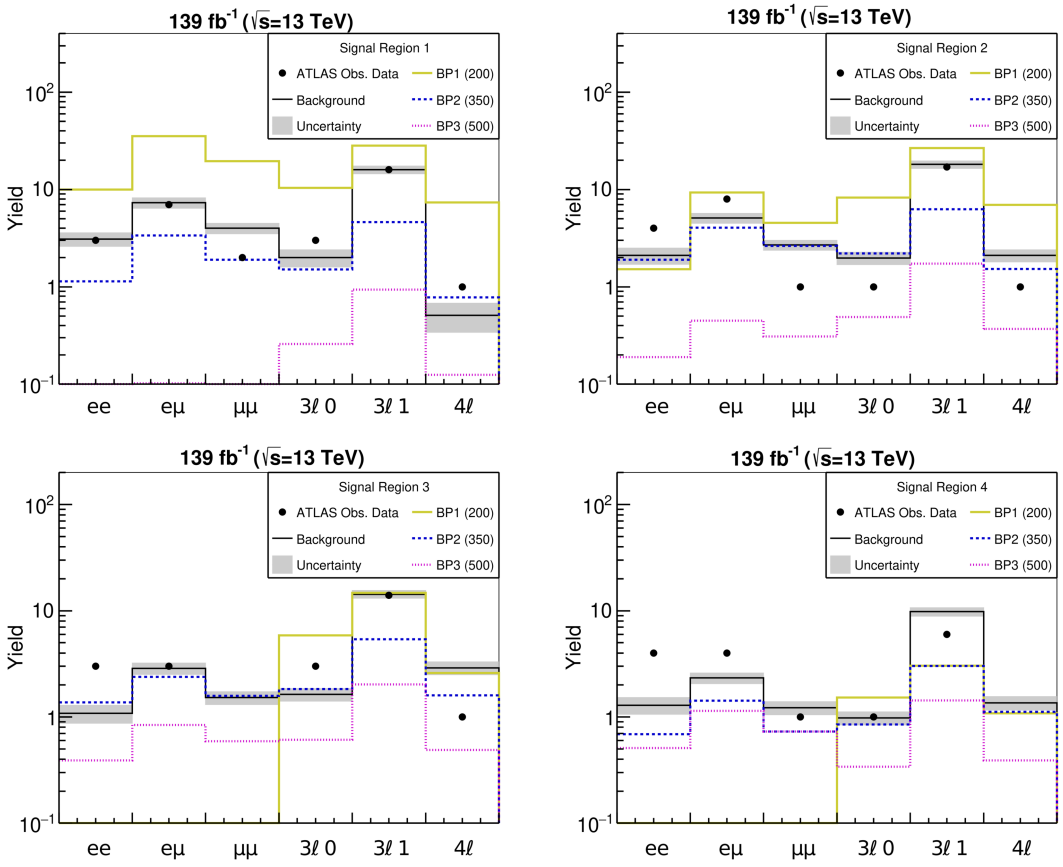

Figure 3. The the expected background, signal and observed events for four different SRs. For each SR, the yields are shown for all the channels. The signal predictions are shown for three benchmark masses. See text for details.

times branching fraction. The green and yellow bands represent the expected exclusion curves within one and two standard deviations, respectively. The NLO QCD corrected [25] theoretical prediction is shown by the solid red curve. The reproduced 95% CL upper limit is represented by the blue dashed curve. The reproduced result is found to be in agreement with the ATLAS one, thereby validating our implementation of this search. This entitles us to use the distributions of expected SM backgrounds and observed events in ref. [82]. Figure 3 shows the expected SM background events(histograms with black line),[13] the observed events (big black dots) and the expected signal events corresponding to 139 fb^{-1} integrated luminosity data at the 13 TeV LHC for four different SRs — *SR1, SR2, SR3* and *SR4*. For each SR, the yields are shown for all the relevant channels, namely ee, $e\mu$, $\mu\mu$, $3\ell 0$, $3\ell 1$ and 4ℓ. The magenta dotted, dark yellow solid and blue dashed histograms show the expected signal events for three benchmark masses — 200, 350 and 500 GeV for $v_t = 1$ GeV and $\Delta m = 0$ assuming NH neutrino mass spectrum with $m_1 = 0.03$ eV.

[13]The gray bands represent the total (systematic + statistical) uncertainty on the expected SM background.

JHEP03(2022)195

Benchmark	Δm (GeV)	v_t (GeV)	$m_{H^{\pm\pm}}$ (GeV)	Exclusion significance (in σ)		
				CMS	ATLAS	Combined
BP1	0	10^{0}	350	0.46	2.54	2.58
BP2	0	10^{-4}	550	1.73	1.03	2.01
BP3	0	10^{-8}	900	2.43	0.24	2.44
BP4	-10	10^{-5}	1050	2.00	0.46	2.05
BP5	10	10^{-5}	200	0.19	0.02	0.19

Table 1. Benchmark points and exclusion significances.

4.3 95% CL lower limit on $m_{H^{\pm\pm}}$

In view of the observations being consistent with the SM background expectations, we derive limits on $m_{H^{\pm\pm}}$ using the LHC searches. In what follows, we present stringent limits with 95% CL on $m_{H^{\pm\pm}}$ for a wide range of v_t and Δm using the above-described CMS multilepton and ATLAS multiboson leading into multilepton searches. In deriving the present limits, we incorporate all the Drell-Yan production modes for the triplet-like scalars. Table 1 displays five benchmark points in different region of the model parameter space along with their exclusion significances from both the CMS and ATLAS searches. Also displayed is the exclusion significances from the CMS and ATLAS combined search. These benchmark points corroborate that the exclusion limits vary significantly across different regions of the v_t–Δm parameter space. The ATLAS and CMS searches fail to probe the triplet-like scalars with mass as low as 200 GeV for the v_t–Δm region characterised by **BP5**, whereas for that characterised by **BP4**, the limit on $m_{H^{\pm\pm}}$ is significantly larger than the previous ones.

The left plot in figure 4 shows 95% CL lower limits on $m_{H^{\pm\pm}}$ as a function of v_t for $\Delta m = 0$ assuming NH neutrino mass spectrum with $m_1 = 0.03$ eV. The khaki shaded region (on the left) is excluded from the ρ parameter measurement from the electroweak precision data, whereas the coral shaded region (on the right) is excluded from the lepton flavour violating decay constraints. The dark goldenrod and pink shaded regions are excluded, respectively, from the CMS multilepton and the ATLAS multiboson leading to multilepton searches. For small v_t, the triplet-like scalars with masses below 950 GeV are excluded from the CMS search. This exclusion limit is stronger than those from the previous LHC searches [78, 79] by approximately 200–230 GeV. For large v_t, the above-described ATLAS search excludes the triplet-like scalars up to 400 GeV masses which is stronger by approximately 50 GeV than the ATLAS limit in ref. [82]. Given that the CMS and ATLAS searches are mutually exclusive, it is reasonable to combine them. That said, as these two searches are primarily designed to target different regions in the parameter space, *viz.* small v_t and large v_t, we expect only marginal improvement on the limits while combining them. The purple shaded region shows excluded parameter space when these two searches are combined.

JHEP03(2022)195

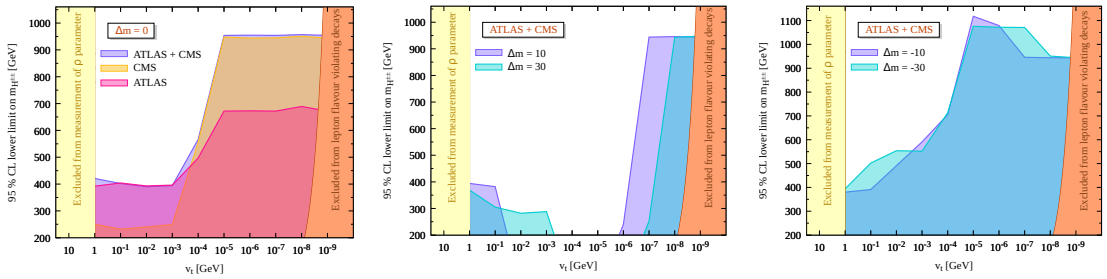

Figure 4. Left: 95% CL lower limits on $m_{H^{\pm\pm}}$ as a function of v_t for $\Delta m = 0$ assuming NH with $m_1 = 0.03\,\text{eV}$. The shaded regions are excluded from different searches at the 13 TeV LHC. Middle(Right): excluded regions from the CMS and ATLAS combined search for $\Delta m = 10$ and 30 (-10 and -30) GeV.

The middle (right) plot in figure 4 shows excluded regions from the CMS and ATLAS combined search for $\Delta m = 10$ and 30 (-10 and -30) GeV. For very large/small v_t, the limits for $\Delta m = \pm 10, \pm 30\,\text{GeV}$ are similar to those for $\Delta m = 0$ case. This is because the cascade decays are yet to open up for very large/small v_t. This makes the non-degenerate scenario identical to the degenerate one. For moderate v_t and large enough Δm, the cascade decays dominate over the other decay modes. In positive scenario, $H^{\pm\pm}$ and $H^{\pm}$ decay into off-shell $W^{\pm}$s (which gives rise to soft jets/leptons) and H^0/A^0 (which further decays invisibly into neutrinos or into $h^0h^0, ZZ/h^0Z$ depending on the value of v_t). For H^0/A^0 decaying into neutrinos, there are hardly visible objects in the final state, so much as the monojet search by ATLAS [112] and the soft leptons search by CMS [115, 116] fall short in constraining this part of the parameter space, see the middle plot in figure 4. On the contrary, for H^0/A^0 decaying into $h^0h^0, ZZ/h^0Z$, the signal cross-section is small compared to the overwhelming background from either QCD jets or Drell-Yan processes. This makes such a scenario challenging to probe. Note that for $v_t \sim \mathcal{O}(10^{-2})$–$\mathcal{O}(10^{-3})$ GeV, the ATLAS search manages to put some bounds in the $\Delta m = 30$ case, but it fails in the $\Delta m = 10$ case. This is because for larger Δm, some of the leptons from the off-shell $W^{\pm}$'s pass the object reconstruction and selection criteria to contribute to the signal yields, whereas the leptons are too soft to do so for smaller Δm. As one approaches towards small v_t, the leptonic decays retrieve their dominance over the cascade one, and give rise to multilepton final states; this occurs at $v_t \sim \mathcal{O}(10^{-6})$ and $\mathcal{O}(10^{-7})$ GeV, respectively, for $\Delta m = 10$ and 30 GeV. This has been reflected in the middle plot. On the contrary, in negative scenario, $H^{\pm}$ and H^0/A^0 decay into off-shell $W^{\pm}$'s and $H^{\pm\pm}$, thereby enhancing the effective production cross-section for $H^{\pm\pm}$. Therefore, in such a scenario, the limit gets enhanced compared to the degenerate case, see the right plot in figure 4. For $\Delta m = -10(-30)$ GeV, the exclusion limit extends up to 1115(1076) GeV compared to 955 GeV for $\Delta m = 0$. Note that for a given $m_{H^{\pm\pm}}$, $H^{\pm}$ and H^0/A^0 are lighter in the $\Delta m = -10$ GeV case compared to those in the $\Delta m = -30$ GeV case. Thus, the signal cross-section is larger for $\Delta m = -10$ GeV than for $\Delta m = -30$ GeV. This explains the stronger limits for $\Delta m = -10$ GeV than $\Delta m = -30$ GeV.

JHEP03(2022)195

4.4 Proposed multilepton final states search for small v_t

For small v_t and $\Delta m = 0$, the triplet-like scalars up to 950 GeV masses are excluded from the CMS multilepton search with 139 fb^{-1} of data, see figure 4. Given the small signal cross-section for $m_{H^{\pm\pm}} > 1$ TeV and comparatively large background in the afore-discussed CMS multilepton search, a similar search at high-luminosity is deemed non-optimal in probing the triplet-like scalars much heavier than 1 TeV. Also, the said search, which results in the most stringent limits in the small v_t region, is not designed to probe the triplet-like scalars. In this section, we design a multilepton search that is optimised to probe the triplet-like scalars much heavier than 1 TeV in the small v_t region. In what follows, we give a brief description about reconstruction and selection of various objects (jets, leptons, etc.), event selection and classification of selected events into mutually exclusive signal regions (SRs) for our proposed multilepton final states search.

Object reconstruction and selection. Different physics objects, *viz.* jets, electrons, muons and missing transverse energy, are reconstructed in `Delphes` [119]. Jets are reconstructed using the anti-kT algorithm [123] with a distance parameter $\Delta R = 0.4$ as implemented in the FastJet package [124]. Reconstructed jets are required to have transverse momentum $p_T > 30$ GeV within the central pseudorapidity range $|\eta| < 2.5$. Electron (muon) candidates with $p_T > 10$ GeV and $|\eta| < 2.5(2.4)$ are considered for further analysis. For the electron candidates within barrel (endcap), we demand a maximum 5-10% (5-15%) p_T-dependent relative isolation with $\Delta R = 0.4$,[14] whereas we demand a maximum 15% relative isolation with $\Delta R = 0.4$ for muons. In addition, the following set of lepton displacement requirements on the transverse and longitudinal impact parameters, d_z and d_{xy}, with respect to the primary vertex are enforced. For electron candidate within barrel (endcap), we demand $d_z < 1$ mm and $d_{xy} < 0.5$ mm ($d_z < 2$ mm and $d_{xy} < 1$ mm), whereas muon candidates require $d_z < 1$ mm and $d_{xy} < 0.5$ mm. Lepton isolation, which trims hadronic activity inside the isolation cone, along with impact parameter requirements suppress the reducible backgrounds such as Z+jets and $t\bar{t}$+jets, where a jet is misidentified as lepton or additional leptons originate from heavy quark decays. Finally, the missing transverse momentum p_T^{miss} is estimated as the magnitude of the negative vector sum of the transverse momenta of all reconstructed particle-flow objects in an event.

Overlaps between reconstructed objects resulting in ambiguities among them lead to object double counting. To sidestep that, all selected jets within a cone of $\Delta R < 0.4$ of a selected lepton are thrown away. In addition, all selected electrons within a cone of $\Delta R < 0.05$ of a selected muon are discarded as these are likely due to bremsstrahlung interactions of the muon with the inner detector material. Some of the jets, especially those on the tail of the detector response, and single pions could mimic lepton signatures and could be misidentified as leptons. Though the composition of the fake-lepton background differs substantially among the analysis channels, without going into the intricacy of modelling the fake-lepton contributions, we straightforwardly take the probability of 0.1–0.3% [125]

[14] The relative isolation is defined as the scalar p_T sum, normalized to the lepton p_T, of photons and hadrons within a cone of ΔR around the lepton. For electrons, this is required to be smaller than $0.0478 + 0.506/p_T$ ($0.0658 + 0.963/p_T$) within barrel (endcap) i.e., $|\eta| < 1.479$ ($|\eta| > 1.479$) with $\Delta R = 0.3$.

JHEP03(2022)195

for a jet to be misidentified as a lepton. Furthermore, bremsstrahlung interactions of the electrons with the inner detector material could lead to charge misidentification. The radiated photon converts to e^-e^+ pair near the primary electron trajectory leading to charge misidentification ambiguity. Also, the photon could traverse the inner detector without creating any track. In such a case, the electron usually has a short lever arm on its curvature. This could lead to incorrect determination of the electron charge. We adopt the charge misidentification probability from ref. [126]: $P(p_T, \eta) = \sigma(p_T) \times f(\eta)$, where $\sigma(p_T)$ is found to be 0.02–0.1 and $f(\eta)$ is found to be 0.03–1 such that $P(p_T, \eta)$ ranges from 0.02% to 10%. Note that the high-p_T electrons are more likely to be affected by charge misidentification as they have almost straight tracks, thereby making the curvature measurement very challenging. Also, the electrons with larger η have a larger misidentification probability as they traverse through a higher amount of inner detector material.

Event selection and signal region definition. Events with three or more light leptons are considered for this search. Events containing a lepton pair with $\Delta R < 0.4$ or a same-flavour lepton pair with invariant mass below 12 GeV are vetoed. This suppresses background contributions from final-state radiations as well as low-mass resonances — Drell-Yan processes and neutral mesons. Furthermore, events containing a same-flavour lepton pair with an invariant mass within the nominal Z-boson mass window, i.e. $M_Z \pm 15$ GeV are discarded.[15] This suppresses background contributions from the $Z \to \ell\ell^* \to \ell\ell\gamma(\to \ell\ell)$ process as well as the WZ production. Events with exactly three light leptons (3L) in one category and four or more light leptons (4L) in another category are considered for further analysis.

Noting that the triplet-like scalars, which are to be probed, are heavier than 1 TeV, we persuade to exploit the relatively high momenta of their decay products. Before continuing, let us briefly reckon the processes contributing to the 3L and 4L signal events. For 3L events, the dominant contribution arises either from the $H^{\pm\pm}H^{\mp} \to \ell^{\pm}\ell^{\pm}\ell^{\mp}\nu$ process or from the $H^{++}H^{--} \to \ell^{\pm}\ell^{\pm}\ell^{\mp}\tau^{\mp}$ process with $\tau^{\pm}$ decaying hadronically. Therefore, the invariant mass distribution of the same-sign lepton pair is expected to peak at $m_{H^{\pm\pm}}$. One would expect high-p_T leptons, large p_T^{miss} and no high-p_T jet (except for those coming from ISR and FSR) in the final states for the former. For the latter, one would expect final states with high-p_T leptons, small p_T^{miss} and at least one high-p_T jet. Then, the dominant contribution to the 4L signal events comes from the $H^{++}H^{--} \to \ell^+\ell^+\ell^-\ell^-$ process. The invariant mass distributions of both the same-sign lepton pairs are expected to peak at $m_{H^{\pm\pm}}$. Once again, one would expect high-p_T leptons and small p_T^{miss} in the final states.

SM backgrounds. A number of SM processes which could mimic the multilepton final states are considered as relevant backgrounds in this analysis. The relevant backgrounds includes ZZ, WZ, WW, Zh, Wh, $t\bar{t}$, $t\bar{t}W$, $t\bar{t}Z$, $t\bar{t}h$, WWW, WWZ, WZZ, ZZZ, ZZh, WWh, $t\bar{t}t(\bar{t})$, $t\bar{t}t\bar{t}$ and Drell-Yan processes. These backgrounds can be classified into two classes — reducible and irreducible backgrounds. The reducible backgrounds are from the

[15] Note that we have relaxed the opposite charge condition for the same-flavour lepton pair to suppress the background contributions due to charge misidentification.

JHEP03(2022)195

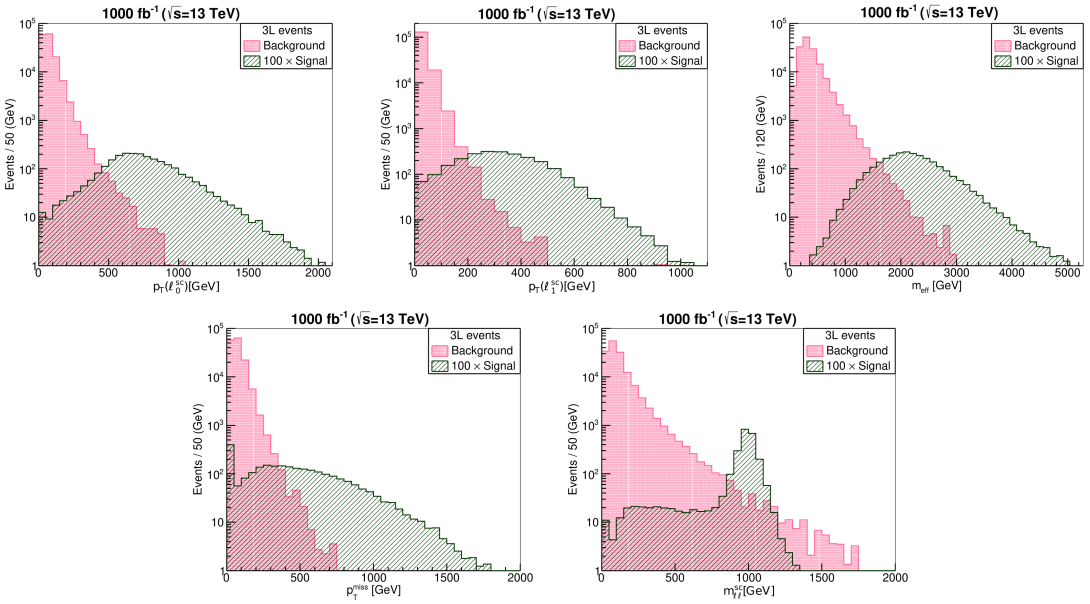

Figure 5. Kinematic distributions for 3L events for **BP1**. Top panel: the p_T-distributions of the leading (leftmost) and subleading (middle) same-charge lepton, and the $m_{\rm eff}$ distribution (rightmost). Bottom panel: the $p_T^{\rm miss}$ (left) and the $m_{\ell\ell}^{\rm sc}$ (right) distributions. The events are weighted at 1000 fb^{-1} luminosity at the 13 TeV LHC.

SM processes like Z/γ^*+jets, $t\bar{t}$+jets, etc., where a jet is misidentified as lepton or additional leptons originate from heavy quark decays. The irreducible ones are from diboson and triboson production and processes like $t\bar{t}W$, $t\bar{t}Z$ and Higgs boson production, etc. Note that final state events with n leptons also contribute to those with $n-1$ leptons when one of the leptons falls outside the detector coverage (in the high rapidity region) or is too soft to pass the object reconstruction and selection criteria or gets misidentified by the detector. All the background events are generated in association of up to two jets using `MadGraph` [96, 97] at the leading order using the 5 flavour scheme followed by MLM matching in `PYTHIA` [118], and the corresponding cross-sections are taken at least upto NLO [127–139].

We plot different kinematic distributions for 3L events in figure 5 for a benchmark point **BP1**, defined as $m_{H^{\pm\pm}} = 1$ TeV, $v_t \sim 10^{-8}$ GeV and $\Delta m = 0$. The first two plots of the top panel show the transverse momentum distributions of the leading and subleading lepton in the same-charge lepton pair. The effective mass, defined as $m_{\rm eff} = H_T + L_T + p_T^{\rm miss}$ with $H_T(L_T)$ being the scalar sum of transverse momenta of all the jets (leptons), distribution is shown in the rightmost plot of the same panel. The bottom panel shows distributions of the missing transverse momentum and the invariant mass of the same-sign lepton pair ($m_{\ell\ell}^{\rm sc}$).[16] These kinematic distributions demonstrate that relatively stronger cuts on the same-sign leptons' p_T and the $m_{\rm eff}$ appreciably reduce the relevant backgrounds. For 3L

[16] In an ideal scenario, the invariant mass distribution in the bottom left plot would have a sharp peak at 1 TeV. However, momentum smearing of the reconstructed objects due to finite resolution of the detectors results in much broader peaks around 1 TeV.

JHEP03(2022)195

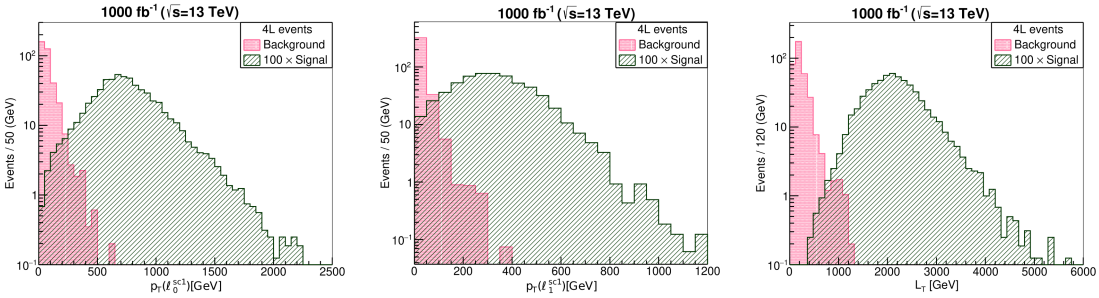

Figure 6. Kinematic distributions for 4L events for **BP1**. Left (middle): the p_T-distributions of the leading (subleading) positive-charge lepton. Right: the L_T distribution. The events are weighted at 1000 fb^{-1} luminosity at the 13 TeV LHC.

events, we require one same-charge lepton pair. The leading (subleading) lepton in the pair is required to have $p_T > 300(100)$ GeV. We discard events with $m_{\text{eff}} < 1500$ GeV. To enhance the sensitivity of this search, the selected events are categorised into two mutually exclusive SRs, namely $3L0J$[17] and $3L1J$, based on whether or not at least one selected jet exists in the event. $3L1J$ events are further classified as $3L1J$-1 and $3L1J$-2 based on whether p_T^{miss} is larger or smaller than 150 GeV. The $3L0J$ events with $p_T^{\text{miss}} < 150$ GeV or $m_{\ell\ell}^{\text{sc}} < 800$ GeV are thrown away to get rid of the sizeable SM backgrounds. Furthermore, we reject $3L1J$-1 events with $p_T^{\text{miss}}/H_T < 1.0$. The cut on p_T^{miss}/H_T turns out to be remarkably effectual in reducing the leftover backgrounds. Finally, to supplement the sensitivity of this search, the selected events in $3L1J$-1 and $3L1J$-2 SRs are divided into six bins each in the [600:1800] GeV range using $m_{\ell\ell}^{\text{sc}}$ as the primary kinematic discriminant.[18]

Different kinematic distributions for 4L events are plotted in figure 6 for **BP1**. The leftmost and middle plot in the top panel shows the transverse momentum distributions of the leading and subleading lepton in the positive-charge lepton pair. The leptons in the negative-charge lepton pair have similar p_T-distributions, we avert to show them for brevity. The distributions of the scalar p_T sum of the leptons is shown in the rightmost plot in the same panel. It is evident from these kinematic distributions that relatively stronger cuts on the same-sign leptons' p_T is useful in suppressing the relevant backgrounds. Further, a cut on L_T turns out to be efficacious in reducing the remaining background. For 4L events, we require two same-charge lepton pairs. The leading (subleading) lepton in both the pairs are required to have $p_T > 300(100)$ GeV. The events with $L_T < 1500$ GeV are vetoed. Further, we require $r = |m_{\ell\ell}^{\text{sc1}} - m_{\ell\ell}^{\text{sc2}}|/(m_{\ell\ell}^{\text{sc1}} + m_{\ell\ell}^{\text{sc2}}) < 0.1$, where $m_{\ell\ell}^{\text{sc1}}$ and $m_{\ell\ell}^{\text{sc2}}$ are the invariant masses of the same-charge lepton pairs. The last cut ensures correct pairing of the leptons.

Number of expected signal and background events in different signal regions after passing various selection cuts for **BP1** for 1000 fb^{-1} of luminosity data at the 13 TeV LHC is are given in table 2. The $3L0J$ and $4L$ signal regions are free from any background, whereas some backgrounds remain after all the selection cuts in the other two signal regions.

[17] Three leptons events with no reconstructed jet with $p_T > 30$ GeV are considered in the $3L0J$ SR.
[18] The overflow (underflow) events are contained in the last (first) bin in each signal region.

JHEP03(2022)195

SR	Selection cuts	Background	Signal
(3L)	Basic	151444	24.9
	$p_T(\ell_0^{\rm sc}) > 300$	1277	23.7
	$p_T(\ell_1^{\rm sc}) > 100$	501	22.7
	$m_{\rm eff} > 1500$	46.0	20.8
$3L0J$	$n_J = 0$ and $p_T^{\rm miss} > 150$	1.0	6.5
	$m_{\ell\ell}^{\rm sc} > 800$	0.0	6.2
$3L1J$-1	$n_J \geq 1$ and $p_T^{\rm miss} > 150$	22.0	10.3
	$p_T^{\rm miss}/H_T > 1.0$	5.1	8.3
$3L1J$-2	$n_J \geq 1$ and $p_T^{\rm miss} < 150$	23.0	3.0

Selection cuts	Background	Signal
Basic	350	6.0
$p_T(\ell_0^{\rm sc1}) > 300$	5.3	5.8
$p_T(\ell_1^{\rm sc1}) > 100$	2.0	5.5
$p_T(\ell_0^{\rm sc2}) > 300$	0.7	5.3
$p_T(\ell_1^{\rm sc2}) > 100$	0.1	5.1
$L_T > 1500$ and $r < 0.1$	0.0	4.9

Table 2. Left (Right): number of expected background and signal events in different 3L (4L) signal regions after passing various selection cuts for **BP1** for 1000 fb^{-1} of luminosity data at the 13 TeV LHC. All the dimensionfull cuts are in GeV.

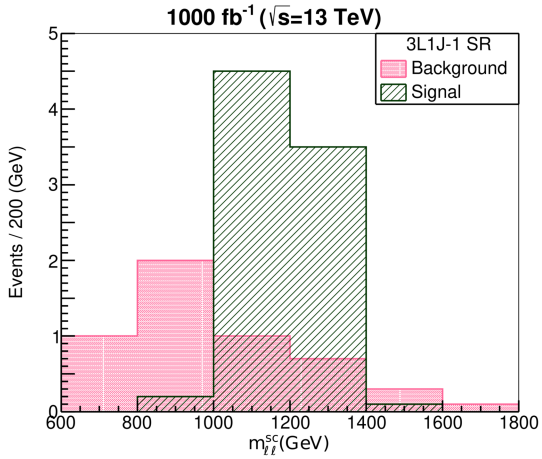

Figure 7. $m_{\ell\ell}^{\rm sc}$ distributions of signal and background events in $3L1J$-1 signal regions after passing various selection cuts for **BP1** for 1000 fb^{-1} of luminosity data at the 13 TeV LHC.

However, these remaining backgrounds are mostly distributed in the lower $m_{\ell\ell}^{\rm sc}$ region unlike the signal events which are distributed in a narrow central $m_{\ell\ell}^{\rm sc}$ region, see figure 7. Figure 7 shows $m_{\ell\ell}^{\rm sc}$ distributions of signal and background events in $3L1J$-1 signal region after passing various selection cuts for **BP1** for 1000 fb^{-1} of luminosity data at the 13 TeV LHC. For brevity, we avert to show similar distribution for the $3L1J$-2 signal region. This simple binning of the selected events enhances sensitivity of these two signal regions.

4.5 Future 95% CL lower limit on $m_{H^{\pm\pm}}$

In this section, we present our forecasted 95% CL lower limits on $m_{H^{\pm\pm}}$ by using the ATLAS search [82] scaled at high-luminosity[19] as well as our proposed search described in section 4.4. We simply presume that not only the detector efficiencies and acceptances

[19]The ATLAS search in ref. [82] is optimised for probing the large v_t region where the type-II see-saw anchors decay into bosons. Thus, we use the same search strategy to forecast the future reach of the LHC in probing this part of the parameter space.

JHEP03(2022)195

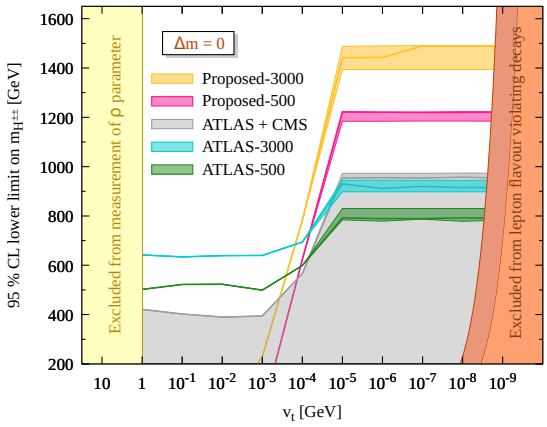

Figure 8. 95% CL lower limits on $m_{H^{\pm\pm}}$ as a function of v_t for $\Delta m = 0$. The gray shaded region is excluded from the existing CMS and ATLAS combined search at the 13 TeV LHC. The bands resulted from different possible neutrino mass hypotheses. See text for details.

but also the background uncertainties remain the same while scaling the ATLAS search at high luminosity. Given that both statistical and systematic contributions to the background uncertainties are expected to be reduced with increasing volume of LHC data, our forecasted limits are conservative. Also, to ensure robustness in statistical interpretations, we replace the less than one per-bin expected background yield at $3000\,\text{fb}^{-1}$,[20] with one background yield. For the proposed search, we assume an overall 20% total uncertainty on the estimated background.

The grey shaded region in figure 8 is excluded from the existing ATLAS and CMS combined search, see section 4.3. The regions below the green and cyan curves are expected to be excluded from the ATLAS search scaled at 500 and $3000\,\text{fb}^{-1}$ of luminosity, respectively. Our proposed search is expected to probe the regions below the goldenrod and pink curves, respectively, at 500 and $3000\,\text{fb}^{-1}$ of luminosity. For small (large) v_t, the future reach extends up to 1220 and 1490 (520 and 640) GeV, respectively, for 500 and $3000\,\text{fb}^{-1}$ of luminosity. We consider both the NH and IH neutrino mass spectrum while varying the lightest neutrino mass in accordance with the bound from cosmology, $\sum_i m_i < 0.12\,\text{eV}$. The effect of different possible neutrino mass hypotheses on the limits are reflected as bands for small v_t regions. This is because, for small v_t, the triplet-like scalars decay leptonically, and these decays are driven by the Yukawa couplings, which, in turn, are determined by the neutrino oscillation parameters up to v_t. For large v_t, the triplet-like scalars decay into diboson and hadrons, and these decays are independent of the Yukawa couplings and the neutrino oscillation parameters. The solid curves within the bands correspond to NH with $m_1 = 0.03\,\text{eV}$. The plots in figure 9 show 95% CL future sensitivity of the LHC to probe as a function of v_t assuming NH with $m_1 = 0.03\,\text{eV}$ for four

[20] All the relevant backgrounds are generated in association of up to two jets using `MadGraph` [96, 97] at the leading order using the 5 flavour scheme followed by MLM matching in `PYTHIA` [118] for $3000\,\text{fb}^{-1}$ or more luminosity, and the corresponding cross-sections are taken at least upto NLO [127–139].

JHEP03(2022)195

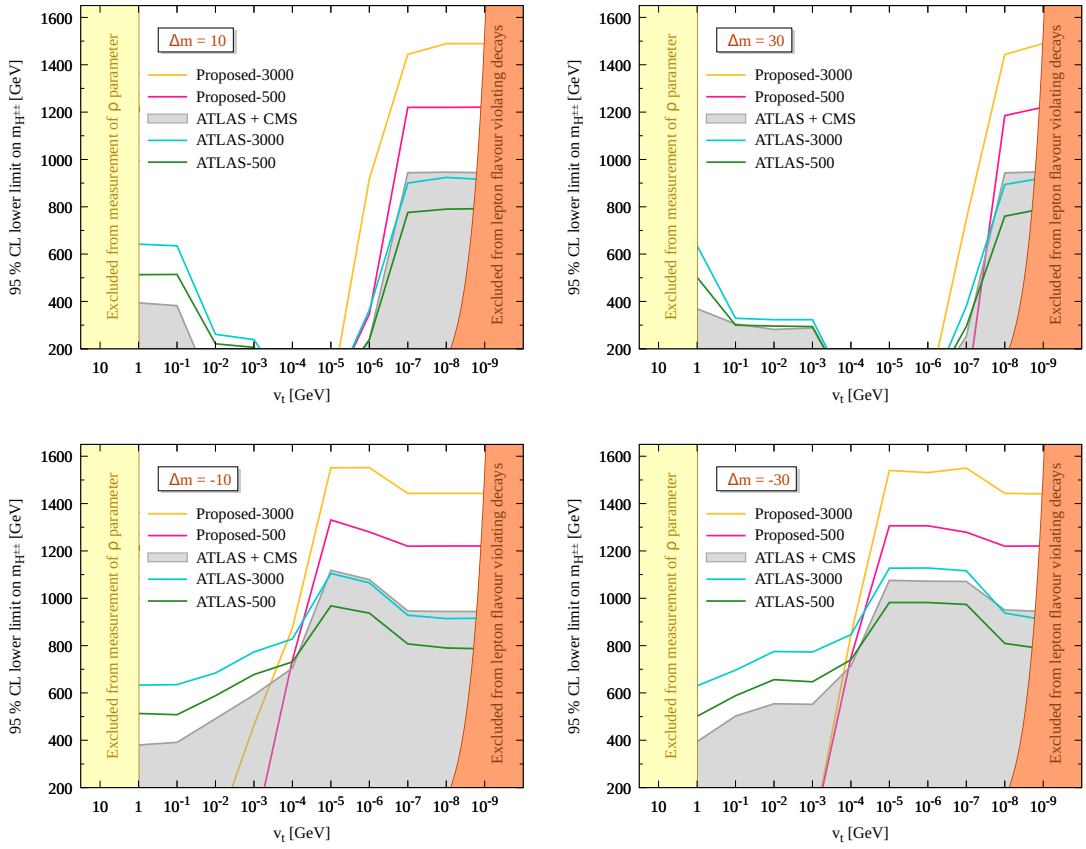

Figure 9. 95% CL lower limits on $m_{H^{\pm\pm}}$ as a function of v_t assuming NH with $m_1 = 0.03\,\text{eV}$ for $\Delta m = 10\,\text{GeV}$ (top left), $\Delta m = 30\,\text{GeV}$ (top right), $\Delta m = -10\,\text{GeV}$ (bottom left) and $\Delta m = -30\,\text{GeV}$ (bottom right). See text for details.

different values of Δm: $\Delta m = 10\,\text{GeV}$ (top left), $\Delta m = 30\,\text{GeV}$ (top right), $\Delta m = -10\,\text{GeV}$ (bottom left) and $\Delta m = -30\,\text{GeV}$ (bottom right). The color codings are same as those in figure 8. For $\Delta m = -10(-30)\,\text{GeV}$ and moderate v_t, the expected reach from our proposed search extends up to 1330(1310) and 1555(1550) GeV, respectively, at 500 and 3000 fb^{-1} of luminiosity.

5 Summary and outlook

The type-II see-saw mechanism based on the annexation of the Standard Model by weak gauge triplet scalar field proffers a natural explanation for the very minuteness of neutrino masses. Because of the presence of the doubly charged scalar bosons and their illustrious signatures, a number of collider searches have been carried out at the LHC by CMS and ATLAS to look for the same. In view of the observations being consistent with the SM background expectations, these searches derived stringent limits with 95% CL on $m_{H^{\pm\pm}}$. Most of these limits are derived in the context of simplified scenarios without reckoning the footprints of the low-energy neutrino parameters. Furthermore, the limits reported

JHEP03(2022)195

by ALTAS and CMS are often conservative as these searches do not incorporate all the Drell-Yan production channels for the triplet-like scalars. As discussed in section 3, other Drell-Yan processes such as pair and associated production of the triplet-like neutral scalars are also of sizeable cross-sections, thus, these too entail to be considered into the analyses. Therefore, the inclusion of these production processes, which are forsaken otherwise by both ATLAS and CMS, results in stronger bounds than those reported by them. Above all, in the non-degenerate scenario, the cascade decays are entitled to play a notable role in the phenomenology, thereby making the phenomenology for the non-degenerate scenario substantially contrasting than that for the degenerate one. Evidently, the ATLAS and CMS reported limits are not befitting to the entire parameter space, rather valid only for a constrained parameter space of the model. Bearing this discussion in mind, we perform a comprehensive study for a wide range of the model parameter space parametrised by v_t, Δm and $m_{H^{\pm\pm}}$. Considering all the Drell-Yan production mechanisms for the triplet-like scalars and taking into account the all-encompassing complexity of their decays, we derive the most stringent 95% CL lower limit on $m_{H^{\pm\pm}}$ for a vast range of v_t-Δm parameter space by implementing already existing direct collider searches by CMS and ATLAS. Further, we forecast future limits by extending the same ATLAS search at high-luminosity, and we propose a search strategy that yields improved limits for a part of the parameter space. To the best of our knowledge, such a study of up-to-the-minute collider limits for a vast range of parameter space is still lacking. This work is intended to fill this gap. In closing this section, we summarise the findings of this work.

(*i*) For $\Delta m = 0$ and large (small) v_t, doubly charged scalars with masses below 420(955) GeV are excluded from the existing ATLAS and CMS combined search. These exclusion limits are approximately 50–230 GeV stronger than those from the previous LHC searches [78, 79, 82]. This is attributed to the inclusion of all the Drell-Yan production processes in our analyses which is not the case for the LHC searches.

(*ii*) For large enough negative Δm and moderate v_t, the recasted limits extend up to 1115 GeV, which is 360–390 GeV stronger than those reported by ATLAS and CMS. In this region of parameter space, $H^{\pm}$ and H^0/A^0 decay to $H^{\pm\pm}$, thereby enhancing the effective production of the latter. This results in improved limits compared to the $\Delta m = 0$ case.

(*iii*) For large enough positive Δm, triplet-like Higgs as light as 200 GeV or even lighter is still allowed by the LHC data. In this region of parameter space, $H^{\pm}$ and $H^{\pm\pm}$ decay to H^0/A^0, thereby enhancing the effective production of H^0/A^0, which then decays invisibly into neutrinos or into $h^0h^0, ZZ/h^0Z$ depending on the value of v_t. For H^0/A^0 decaying into neutrinos, there are hardly visible objects in the final state, so much as the monojet search by ATLAS [112] and the soft leptons search by CMS [115, 116] fall short in constraining this part of the parameter space. On the contrary, for H^0/A^0 decaying into $h^0h^0, ZZ/h^0Z$, the signal cross-section is small compared to the overwhelming background either from QCD jets or Drell-Yan processes. This makes

JHEP03(2022)195

such a scenario challenging to probe at the LHC. Note that e^-e^+ colliders could have better prospects for probing such a nightmare scenario, which we left for future work.

(*iv*) For $\Delta m = 0$ and large v_t, the expected reach of the ATLAS search at $3000\,\text{fb}^{-1}$ is 640 GeV.

(*v*) For $\Delta m = 0$ and small v_t, the expected reach from our proposed search extends up to 1490 GeV at $3000\,\text{fb}^{-1}$, while for $\Delta m = -10(-30)$ GeV and moderate v_t, the reach is 1555(1550) GeV.

Acknowledgments

KG acknowledges the support from the DST/INSPIRE Research Grant [DST/INSPIRE/04/2014/002158] and SERB Core Research Grant [CRG/2019/006831]. The simulations were supported in part by the SAMKHYA: High Performance Computing Facility provided by Institute of Physics, Bhubaneswar.

References

[1] W. Konetschny and W. Kummer, *Nonconservation of Total Lepton Number with Scalar Bosons*, *Phys. Lett. B* **70** (1977) 433 [INSPIRE].

[2] T.P. Cheng and L.-F. Li, *Neutrino Masses, Mixings and Oscillations in* SU(2) × U(1) *Models of Electroweak Interactions*, *Phys. Rev. D* **22** (1980) 2860 [INSPIRE].

[3] G. Lazarides, Q. Shafi and C. Wetterich, *Proton Lifetime and Fermion Masses in an* SO(10) *Model*, *Nucl. Phys. B* **181** (1981) 287 [INSPIRE].

[4] J. Schechter and J.W.F. Valle, *Neutrino Masses in* SU(2) × U(1) *Theories*, *Phys. Rev. D* **22** (1980) 2227 [INSPIRE].

[5] R.N. Mohapatra and G. Senjanović, *Neutrino Masses and Mixings in Gauge Models with Spontaneous Parity Violation*, *Phys. Rev. D* **23** (1981) 165 [INSPIRE].

[6] M. Magg and C. Wetterich, *Neutrino Mass Problem and Gauge Hierarchy*, *Phys. Lett. B* **94** (1980) 61 [INSPIRE].

[7] A. Arhrib et al., *The Higgs Potential in the Type II Seesaw Model*, *Phys. Rev. D* **84** (2011) 095005 [arXiv:1105.1925] [INSPIRE].

[8] F. Arbabifar, S. Bahrami and M. Frank, *Neutral Higgs Bosons in the Higgs Triplet Model with nontrivial mixing*, *Phys. Rev. D* **87** (2013) 015020 [arXiv:1211.6797] [INSPIRE].

[9] E.J. Chun, H.M. Lee and P. Sharma, *Vacuum Stability, Perturbativity, EWPD and Higgs-to-diphoton rate in Type II Seesaw Models*, *JHEP* **11** (2012) 106 [arXiv:1209.1303] [INSPIRE].

[10] P.S. Bhupal Dev, D.K. Ghosh, N. Okada and I. Saha, *125 GeV Higgs Boson and the Type-II Seesaw Model*, *JHEP* **03** (2013) 150 [*Erratum ibid.* **05** (2013) 049] [arXiv:1301.3453] [INSPIRE].

JHEP03(2022)195

[11] D. Das and A. Santamaria, *Updated scalar sector constraints in the Higgs triplet model*, *Phys. Rev. D* **94** (2016) 015015 [arXiv:1604.08099] [INSPIRE].

[12] M.L. Swartz, *Limits on Doubly Charged Higgs Bosons and Lepton Flavor Violation*, *Phys. Rev. D* **40** (1989) 1521 [INSPIRE].

[13] M. Kakizaki, Y. Ogura and F. Shima, *Lepton flavor violation in the triplet Higgs model*, *Phys. Lett. B* **566** (2003) 210 [hep-ph/0304254] [INSPIRE].

[14] A.G. Akeroyd, M. Aoki and H. Sugiyama, *Lepton Flavour Violating Decays $\tau \to \bar{\ell}\ell\ell$ and $\mu \to e\gamma$ in the Higgs Triplet Model*, *Phys. Rev. D* **79** (2009) 113010 [arXiv:0904.3640] [INSPIRE].

[15] D.N. Dinh, A. Ibarra, E. Molinaro and S.T. Petcov, *The $\mu - e$ Conversion in Nuclei, $\mu \to e\gamma, \mu \to 3e$ Decays and TeV Scale See-Saw Scenarios of Neutrino Mass Generation*, *JHEP* **08** (2012) 125 [*Erratum ibid.* **09** (2013) 023] [arXiv:1205.4671] [INSPIRE].

[16] G. Bambhaniya, P.S.B. Dev, S. Goswami and M. Mitra, *The Scalar Triplet Contribution to Lepton Flavour Violation and Neutrinoless Double Beta Decay in Left-Right Symmetric Model*, *JHEP* **04** (2016) 046 [arXiv:1512.00440] [INSPIRE].

[17] J. Chakrabortty, P. Ghosh, S. Mondal and T. Srivastava, *Reconciling $(g-2)_\mu$ and charged lepton flavor violating processes through a doubly charged scalar*, *Phys. Rev. D* **93** (2016) 115004 [arXiv:1512.03581] [INSPIRE].

[18] E.J. Chun, K.Y. Lee and S.C. Park, *Testing Higgs triplet model and neutrino mass patterns*, *Phys. Lett. B* **566** (2003) 142 [hep-ph/0304069] [INSPIRE].

[19] J. Garayoa and T. Schwetz, *Neutrino mass hierarchy and Majorana CP phases within the Higgs triplet model at the LHC*, *JHEP* **03** (2008) 009 [arXiv:0712.1453] [INSPIRE].

[20] M. Kadastik, M. Raidal and L. Rebane, *Direct determination of neutrino mass parameters at future colliders*, *Phys. Rev. D* **77** (2008) 115023 [arXiv:0712.3912] [INSPIRE].

[21] A.G. Akeroyd, M. Aoki and H. Sugiyama, *Probing Majorana Phases and Neutrino Mass Spectrum in the Higgs Triplet Model at the CERN LHC*, *Phys. Rev. D* **77** (2008) 075010 [arXiv:0712.4019] [INSPIRE].

[22] P. Fileviez Perez, T. Han, G.-y. Huang, T. Li and K. Wang, *Neutrino Masses and the CERN LHC: Testing Type II Seesaw*, *Phys. Rev. D* **78** (2008) 015018 [arXiv:0805.3536] [INSPIRE].

[23] K. Huitu, J. Maalampi, A. Pietila and M. Raidal, *Doubly charged Higgs at LHC*, *Nucl. Phys. B* **487** (1997) 27 [hep-ph/9606311] [INSPIRE].

[24] J.F. Gunion, C. Loomis and K.T. Pitts, *Searching for doubly charged Higgs bosons at future colliders*, *eConf* **C 960625** (1996) LTH096 [hep-ph/9610237] [INSPIRE].

[25] M. Muhlleitner and M. Spira, *A Note on doubly charged Higgs pair production at hadron colliders*, *Phys. Rev. D* **68** (2003) 117701 [hep-ph/0305288] [INSPIRE].

[26] A.G. Akeroyd and M. Aoki, *Single and pair production of doubly charged Higgs bosons at hadron colliders*, *Phys. Rev. D* **72** (2005) 035011 [hep-ph/0506176] [INSPIRE].

[27] T. Han, B. Mukhopadhyaya, Z. Si and K. Wang, *Pair production of doubly-charged scalars: Neutrino mass constraints and signals at the LHC*, *Phys. Rev. D* **76** (2007) 075013 [arXiv:0706.0441] [INSPIRE].

JHEP03(2022)195

[28] F. del Aguila and J.A. Aguilar-Saavedra, *Distinguishing seesaw models at LHC with multi-lepton signals*, *Nucl. Phys. B* **813** (2009) 22 [arXiv:0808.2468] [INSPIRE].

[29] A.G. Akeroyd and C.-W. Chiang, *Doubly charged Higgs bosons and three-lepton signatures in the Higgs Triplet Model*, *Phys. Rev. D* **80** (2009) 113010 [arXiv:0909.4419] [INSPIRE].

[30] A.G. Akeroyd, C.-W. Chiang and N. Gaur, *Leptonic signatures of doubly charged Higgs boson production at the LHC*, *JHEP* **11** (2010) 005 [arXiv:1009.2780] [INSPIRE].

[31] C.-W. Chiang, T. Nomura and K. Tsumura, *Search for doubly charged Higgs bosons using the same-sign diboson mode at the LHC*, *Phys. Rev. D* **85** (2012) 095023 [arXiv:1202.2014] [INSPIRE].

[32] S. Kanemura, K. Yagyu and H. Yokoya, *First constraint on the mass of doubly-charged Higgs bosons in the same-sign diboson decay scenario at the LHC*, *Phys. Lett. B* **726** (2013) 316 [arXiv:1305.2383] [INSPIRE].

[33] Z. Kang, J. Li, T. Li, Y. Liu and G.-Z. Ning, *Light Doubly Charged Higgs Boson via the WW^* Channel at LHC*, *Eur. Phys. J. C* **75** (2015) 574 [arXiv:1404.5207] [INSPIRE].

[34] S. Kanemura, M. Kikuchi, K. Yagyu and H. Yokoya, *Bounds on the mass of doubly-charged Higgs bosons in the same-sign diboson decay scenario*, *Phys. Rev. D* **90** (2014) 115018 [arXiv:1407.6547] [INSPIRE].

[35] S. Kanemura, M. Kikuchi, H. Yokoya and K. Yagyu, *LHC Run-I constraint on the mass of doubly charged Higgs bosons in the same-sign diboson decay scenario*, *PTEP* **2015** (2015) 051B02 [arXiv:1412.7603] [INSPIRE].

[36] T.B. de Melo, F.S. Queiroz and Y. Villamizar, *Doubly Charged Scalar at the High-Luminosity and High-Energy LHC*, *Int. J. Mod. Phys. A* **34** (2019) 1950157 [arXiv:1909.07429] [INSPIRE].

[37] R. Padhan, D. Das, M. Mitra and A. Kumar Nayak, *Probing doubly and singly charged Higgs bosons at the pp collider HE-LHC*, *Phys. Rev. D* **101** (2020) 075050 [arXiv:1909.10495] [INSPIRE].

[38] S. Chakrabarti, D. Choudhury, R.M. Godbole and B. Mukhopadhyaya, *Observing doubly charged Higgs bosons in photon-photon collisions*, *Phys. Lett. B* **434** (1998) 347 [hep-ph/9804297] [INSPIRE].

[39] A. Melfo, M. Nemevšek, F. Nesti, G. Senjanović and Y. Zhang, *Type II Seesaw at LHC: The Roadmap*, *Phys. Rev. D* **85** (2012) 055018 [arXiv:1108.4416] [INSPIRE].

[40] M. Aoki, S. Kanemura and K. Yagyu, *Testing the Higgs triplet model with the mass difference at the LHC*, *Phys. Rev. D* **85** (2012) 055007 [arXiv:1110.4625] [INSPIRE].

[41] A.G. Akeroyd and H. Sugiyama, *Production of doubly charged scalars from the decay of singly charged scalars in the Higgs Triplet Model*, *Phys. Rev. D* **84** (2011) 035010 [arXiv:1105.2209] [INSPIRE].

[42] A.G. Akeroyd, S. Moretti and H. Sugiyama, *Five-lepton and six-lepton signatures from production of neutral triplet scalars in the Higgs Triplet Model*, *Phys. Rev. D* **85** (2012) 055026 [arXiv:1201.5047] [INSPIRE].

[43] E.J. Chun and P. Sharma, *Same-Sign Tetra-Leptons from Type II Seesaw*, *JHEP* **08** (2012) 162 [arXiv:1206.6278] [INSPIRE].

JHEP03(2022)195

[44] E.J. Chun and P. Sharma, *Search for a doubly-charged boson in four lepton final states in type-II seesaw*, *Phys. Lett. B* **728** (2014) 256 [arXiv:1309.6888] [INSPIRE].

[45] Z.-L. Han, R. Ding and Y. Liao, *LHC Phenomenology of Type II Seesaw: Nondegenerate Case*, *Phys. Rev. D* **91** (2015) 093006 [arXiv:1502.05242] [INSPIRE].

[46] Z.-L. Han, R. Ding and Y. Liao, *LHC phenomenology of the type-II seesaw mechanism: Observability of neutral scalars in the nondegenerate case*, *Phys. Rev. D* **92** (2015) 033014 [arXiv:1506.08996] [INSPIRE].

[47] M. Mitra, S. Niyogi and M. Spannowsky, *Type-II Seesaw Model and Multilepton Signatures at Hadron Colliders*, *Phys. Rev. D* **95** (2017) 035042 [arXiv:1611.09594] [INSPIRE].

[48] D.K. Ghosh, N. Ghosh, I. Saha and A. Shaw, *Revisiting the high-scale validity of the type-II seesaw model with novel LHC signature*, *Phys. Rev. D* **97** (2018) 115022 [arXiv:1711.06062] [INSPIRE].

[49] R. Primulando, J. Julio and P. Uttayarat, *Scalar phenomenology in type-II seesaw model*, *JHEP* **08** (2019) 024 [arXiv:1903.02493] [INSPIRE].

[50] E.J. Chun, S. Khan, S. Mandal, M. Mitra and S. Shil, *Same-sign tetralepton signature at the Large Hadron Collider and a future pp collider*, *Phys. Rev. D* **101** (2020) 075008 [arXiv:1911.00971] [INSPIRE].

[51] S. Antusch, O. Fischer, A. Hammad and C. Scherb, *Low scale type-II seesaw: Present constraints and prospects for displaced vertex searches*, *JHEP* **02** (2019) 157 [arXiv:1811.03476] [INSPIRE].

[52] P.S. Bhupal Dev and Y. Zhang, *Displaced vertex signatures of doubly charged scalars in the type-II seesaw and its left-right extensions*, *JHEP* **10** (2018) 199 [arXiv:1808.00943] [INSPIRE].

[53] Y. Cai, T. Han, T. Li and R. Ruiz, *Lepton Number Violation: Seesaw Models and Their Collider Tests*, *Front. in Phys.* **6** (2018) 40 [arXiv:1711.02180] [INSPIRE].

[54] F.F. Deppisch, P.S. Bhupal Dev and A. Pilaftsis, *Neutrinos and Collider Physics*, *New J. Phys.* **17** (2015) 075019 [arXiv:1502.06541] [INSPIRE].

[55] J.C. Pati and A. Salam, *Lepton Number as the Fourth Color*, *Phys. Rev. D* **10** (1974) 275 [*Erratum ibid.* **11** (1975) 703] [INSPIRE].

[56] R.N. Mohapatra and J.C. Pati, *Left-Right Gauge Symmetry and an Isoconjugate Model of CP-violation*, *Phys. Rev. D* **11** (1975) 566 [INSPIRE].

[57] G. Senjanović and R.N. Mohapatra, *Exact Left-Right Symmetry and Spontaneous Violation of Parity*, *Phys. Rev. D* **12** (1975) 1502 [INSPIRE].

[58] J.F. Gunion, R. Vega and J. Wudka, *Higgs triplets in the standard model*, *Phys. Rev. D* **42** (1990) 1673 [INSPIRE].

[59] J.E. Cieza Montalvo, N.V. Cortez, J. Sa Borges and M.D. Tonasse, *Searching for doubly charged Higgs bosons at the LHC in a 3-3-1 model*, *Nucl. Phys. B* **756** (2006) 1 [*Erratum ibid.* **796** (2008) 422] [hep-ph/0606243] [INSPIRE].

[60] N. Arkani-Hamed, A.G. Cohen, E. Katz, A.E. Nelson, T. Gregoire and J.G. Wacker, *The Minimal moose for a little Higgs*, *JHEP* **08** (2002) 021 [hep-ph/0206020] [INSPIRE].

[61] N. Arkani-Hamed, A.G. Cohen, E. Katz and A.E. Nelson, *The Littlest Higgs*, *JHEP* **07** (2002) 034 [hep-ph/0206021] [INSPIRE].

JHEP03(2022)195

[62] A. Hektor, M. Kadastik, M. Muntel, M. Raidal and L. Rebane, *Testing neutrino masses in little Higgs models via discovery of doubly charged Higgs at LHC*, *Nucl. Phys. B* **787** (2007) 198 [arXiv:0705.1495] [INSPIRE].

[63] M.S. Chanowitz and M. Golden, *Higgs Boson Triplets With $M_W = M_Z \cos\theta_W$*, *Phys. Lett. B* **165** (1985) 105 [INSPIRE].

[64] H. Georgi and M. Machacek, *Doubly charged Higgs bosons*, *Nucl. Phys. B* **262** (1985) 463 [INSPIRE].

[65] A. Zee, *Quantum Numbers of Majorana Neutrino Masses*, *Nucl. Phys. B* **264** (1986) 99 [INSPIRE].

[66] K.S. Babu, *Model of 'Calculable' Majorana Neutrino Masses*, *Phys. Lett. B* **203** (1988) 132 [INSPIRE].

[67] K.S. Babu, S. Nandi and Z. Tavartkiladze, *New Mechanism for Neutrino Mass Generation and Triply Charged Higgs Bosons at the LHC*, *Phys. Rev. D* **80** (2009) 071702 [arXiv:0905.2710] [INSPIRE].

[68] I. Picek and B. Radovcic, *Novel TeV-scale seesaw mechanism with Dirac mediators*, *Phys. Lett. B* **687** (2010) 338 [arXiv:0911.1374] [INSPIRE].

[69] K. Kumericki, I. Picek and B. Radovcic, *TeV-scale Seesaw with Quintuplet Fermions*, *Phys. Rev. D* **86** (2012) 013006 [arXiv:1204.6599] [INSPIRE].

[70] R. Cepedello, M. Hirsch and J.C. Helo, *Lepton number violating phenomenology of $d = 7$ neutrino mass models*, *JHEP* **01** (2018) 009 [arXiv:1709.03397] [INSPIRE].

[71] G. Anamiati, O. Castillo-Felisola, R.M. Fonseca, J.C. Helo and M. Hirsch, *High-dimensional neutrino masses*, *JHEP* **12** (2018) 066 [arXiv:1806.07264] [INSPIRE].

[72] Avnish and K. Ghosh, *Multi-charged TeV scale scalars and fermions in the framework of a radiative seesaw model*, arXiv:2007.01766 [INSPIRE].

[73] ATLAS collaboration, *Search for doubly-charged Higgs bosons in like-sign dilepton final states at $\sqrt{s} = 7$ TeV with the ATLAS detector*, *Eur. Phys. J. C* **72** (2012) 2244 [arXiv:1210.5070] [INSPIRE].

[74] CMS collaboration, *A Search for a Doubly-Charged Higgs Boson in pp Collisions at $\sqrt{s} = 7$ TeV*, *Eur. Phys. J. C* **72** (2012) 2189 [arXiv:1207.2666] [INSPIRE].

[75] ATLAS collaboration, *Search for anomalous production of prompt same-sign lepton pairs and pair-produced doubly charged Higgs bosons with $\sqrt{s} = 8$ TeV pp collisions using the ATLAS detector*, *JHEP* **03** (2015) 041 [arXiv:1412.0237] [INSPIRE].

[76] CMS collaboration, *Study of vector boson scattering and search for new physics in events with two same-sign leptons and two jets*, *Phys. Rev. Lett.* **114** (2015) 051801 [arXiv:1410.6315] [INSPIRE].

[77] CMS collaboration, *Search for a doubly-charged Higgs boson with $\sqrt{s} = 8$ TeV pp collisions at the CMS experiment*, CMS-PAS-HIG-14-039 (2014).

[78] CMS collaboration, *A search for doubly-charged Higgs boson production in three and four lepton final states at $\sqrt{s} = 13$ TeV*, CMS-PAS-HIG-16-036 (2016).

[79] ATLAS collaboration, *Search for doubly charged Higgs boson production in multi-lepton final states with the ATLAS detector using proton–proton collisions at $\sqrt{s} = 13$ TeV*, *Eur. Phys. J. C* **78** (2018) 199 [arXiv:1710.09748] [INSPIRE].

JHEP03(2022)195

[80] CMS collaboration, *Observation of electroweak production of same-sign W boson pairs in the two jet and two same-sign lepton final state in proton-proton collisions at* $\sqrt{s} = 13$ *TeV*, *Phys. Rev. Lett.* **120** (2018) 081801 [arXiv:1709.05822] [INSPIRE].

[81] ATLAS collaboration, *Search for doubly charged scalar bosons decaying into same-sign W boson pairs with the ATLAS detector*, *Eur. Phys. J. C* **79** (2019) 58 [arXiv:1808.01899] [INSPIRE].

[82] ATLAS collaboration, *Search for doubly and singly charged Higgs bosons decaying into vector bosons in multi-lepton final states with the ATLAS detector using proton-proton collisions at* $\sqrt{s} = 13$ *TeV*, *JHEP* **06** (2021) 146 [arXiv:2101.11961] [INSPIRE].

[83] M. Cirelli, N. Fornengo and A. Strumia, *Minimal dark matter*, *Nucl. Phys. B* **753** (2006) 178 [hep-ph/0512090] [INSPIRE].

[84] PLANCK collaboration, *Planck 2018 results. VI. Cosmological parameters*, *Astron. Astrophys.* **641** (2020) A6 [*Erratum ibid.* **652** (2021) C4] [arXiv:1807.06209] [INSPIRE].

[85] I. Esteban, M.C. Gonzalez-Garcia, M. Maltoni, T. Schwetz and A. Zhou, *The fate of hints: updated global analysis of three-flavor neutrino oscillations*, *JHEP* **09** (2020) 178 [arXiv:2007.14792] [INSPIRE].

[86] PARTICLE DATA GROUP collaboration, *Review of Particle Physics*, *PTEP* **2020** (2020) 083C01 [INSPIRE].

[87] M. Aoki, S. Kanemura, M. Kikuchi and K. Yagyu, *Radiative corrections to the Higgs boson couplings in the triplet model*, *Phys. Rev. D* **87** (2013) 015012 [arXiv:1211.6029] [INSPIRE].

[88] MEG collaboration, *Search for the lepton flavour violating decay* $\mu^+ \to e^+\gamma$ *with the full dataset of the MEG experiment*, *Eur. Phys. J. C* **76** (2016) 434 [arXiv:1605.05081] [INSPIRE].

[89] SINDRUM collaboration, *Search for the Decay* $\mu^+ \to e^+e^+e^-$, *Nucl. Phys. B* **299** (1988) 1 [INSPIRE].

[90] K.S. Babu and S. Jana, *Probing Doubly Charged Higgs Bosons at the LHC through Photon Initiated Processes*, *Phys. Rev. D* **95** (2017) 055020 [arXiv:1612.09224] [INSPIRE].

[91] K. Ghosh, S. Jana and S. Nandi, *Neutrino Mass Generation at TeV Scale and New Physics Signatures from Charged Higgs at the LHC for Photon Initiated Processes*, *JHEP* **03** (2018) 180 [arXiv:1705.01121] [INSPIRE].

[92] F. del Águila and M. Chala, *LHC bounds on Lepton Number Violation mediated by doubly and singly-charged scalars*, *JHEP* **03** (2014) 027 [arXiv:1311.1510] [INSPIRE].

[93] B. Dutta, R. Eusebi, Y. Gao, T. Ghosh and T. Kamon, *Exploring the doubly charged Higgs boson of the left-right symmetric model using vector boson fusionlike events at the LHC*, *Phys. Rev. D* **90** (2014) 055015 [arXiv:1404.0685] [INSPIRE].

[94] F. Staub, *SARAH 4: A tool for (not only SUSY) model builders*, *Comput. Phys. Commun.* **185** (2014) 1773 [arXiv:1309.7223] [INSPIRE].

[95] F. Staub, *Exploring new models in all detail with SARAH*, *Adv. High Energy Phys.* **2015** (2015) 840780 [arXiv:1503.04200] [INSPIRE].

[96] J. Alwall, M. Herquet, F. Maltoni, O. Mattelaer and T. Stelzer, *MadGraph 5: Going Beyond*, *JHEP* **06** (2011) 128 [arXiv:1106.0522] [INSPIRE].

JHEP03(2022)195

[97] J. Alwall et al., *The automated computation of tree-level and next-to-leading order differential cross sections, and their matching to parton shower simulations*, *JHEP* **07** (2014) 079 [arXiv:1405.0301] [INSPIRE].

[98] NNPDF collaboration, *Parton distributions with QED corrections*, *Nucl. Phys. B* **877** (2013) 290 [arXiv:1308.0598] [INSPIRE].

[99] NNPDF collaboration, *Parton distributions for the LHC Run II*, *JHEP* **04** (2015) 040 [arXiv:1410.8849] [INSPIRE].

[100] B. Fuks, M. Nemevšek and R. Ruiz, *Doubly Charged Higgs Boson Production at Hadron Colliders*, *Phys. Rev. D* **101** (2020) 075022 [arXiv:1912.08975] [INSPIRE].

[101] T.G. Rizzo, *Decays of Heavy Higgs Bosons*, *Phys. Rev. D* **22** (1980) 722 [INSPIRE].

[102] W.-Y. Keung and W.J. Marciano, *Higgs-scalar decays: $H \to W^{\pm} + X$*, *Phys. Rev. D* **30** (1984) 248 [INSPIRE].

[103] R.N. Cahn, *A Higgs primer*, in *GIF 90: 22nd Summer School on Particle Physics: Where is the Higgs?*, Strasbourg, France (1990), Report number: LBL-29789.

[104] A. Djouadi, *Decays of the Higgs bosons*, in *International Workshop on Quantum Effects in the Minimal Supersymmetric Standard Model*, Barcelona, Spain (1997), pg. 197 [hep-ph/9712334] [INSPIRE].

[105] S. Banerjee, M. Frank and S.K. Rai, *Higgs data confronts Sequential Fourth Generation Fermions in the Higgs Triplet Model*, *Phys. Rev. D* **89** (2014) 075005 [arXiv:1312.4249] [INSPIRE].

[106] A. Crivellin, M. Ghezzi, L. Panizzi, G.M. Pruna and A. Signer, *Low- and high-energy phenomenology of a doubly charged scalar*, *Phys. Rev. D* **99** (2019) 035004 [arXiv:1807.10224] [INSPIRE].

[107] Y. Du, A. Dunbrack, M.J. Ramsey-Musolf and J.-H. Yu, *Type-II Seesaw Scalar Triplet Model at a 100 TeV pp Collider: Discovery and Higgs Portal Coupling Determination*, *JHEP* **01** (2019) 101 [arXiv:1810.09450] [INSPIRE].

[108] P.S. Bhupal Dev and Y. Zhang, *Displaced vertex signatures of doubly charged scalars in the type-II seesaw and its left-right extensions*, *JHEP* **10** (2018) 199 [arXiv:1808.00943] [INSPIRE].

[109] A. Aboubrahim and P. Nath, *Naturalness, the hyperbolic branch, and prospects for the observation of charged Higgs bosons at high luminosity LHC and 27 TeV LHC*, *Phys. Rev. D* **98** (2018) 095024 [arXiv:1810.12868] [INSPIRE].

[110] CMS collaboration, *Search for physics beyond the standard model in multilepton final states in proton-proton collisions at $\sqrt{s} = 13$ TeV*, *JHEP* **03** (2020) 051 [arXiv:1911.04968] [INSPIRE].

[111] ATLAS collaboration, *Search for new phenomena in three- or four-lepton events in pp collisions at $\sqrt{s} = 13$ TeV with the ATLAS detector*, ATLAS-CONF-2021-011 (2021).

[112] ATLAS collaboration, *Search for new phenomena in events with an energetic jet and missing transverse momentum in pp collisions at $\sqrt{s} = 13$ TeV with the ATLAS detector*, *Phys. Rev. D* **103** (2021) 112006 [arXiv:2102.10874] [INSPIRE].

JHEP03(2022)195

[113] ATLAS collaboration, *Search for new phenomena in final states with an energetic jet and large missing transverse momentum in pp collisions at $\sqrt{s} = 13$ TeV using the ATLAS detector*, *Phys. Rev. D* **94** (2016) 032005 [arXiv:1604.07773] [INSPIRE].

[114] ATLAS collaboration, *Search for dark matter and other new phenomena in events with an energetic jet and large missing transverse momentum using the ATLAS detector*, *JHEP* **01** (2018) 126 [arXiv:1711.03301] [INSPIRE].

[115] CMS collaboration, *Search for physics beyond the standard model in final states with two or three soft leptons and missing transverse momentum in proton-proton collisions at 13 TeV*, CMS-PAS-SUS-18-004 (2018).

[116] CMS collaboration, *Search for new physics in events with two soft oppositely charged leptons and missing transverse momentum in proton-proton collisions at $\sqrt{s} = 13$ TeV*, *Phys. Lett. B* **782** (2018) 440 [arXiv:1801.01846] [INSPIRE].

[117] R. Foot, H. Lew, X.G. He and G.C. Joshi, *Seesaw Neutrino Masses Induced by a Triplet of Leptons*, *Z. Phys. C* **44** (1989) 441 [INSPIRE].

[118] T. Sjöstrand et al., *An introduction to PYTHIA 8.2*, *Comput. Phys. Commun.* **191** (2015) 159 [arXiv:1410.3012] [INSPIRE].

[119] DELPHES 3 collaboration, *DELPHES 3, A modular framework for fast simulation of a generic collider experiment*, *JHEP* **02** (2014) 057 [arXiv:1307.6346] [INSPIRE].

[120] W. Verkerke and D.P. Kirkby, *The RooFit toolkit for data modeling*, *eConf* **C 0303241** (2003) MOLT007 [physics/0306116] [INSPIRE].

[121] S. Ashanujjaman and K. Ghosh, *A genuine fermionic quintuplet seesaw model: phenomenological introduction*, *JHEP* **06** (2021) 084 [arXiv:2012.15609] [INSPIRE].

[122] S. Ashanujjaman and K. Ghosh, *Type-III see-saw: Phenomenological implications of the information lost in decoupling from high-energy to low-energy*, *Phys. Lett. B* **819** (2021) 136403 [arXiv:2102.09536] [INSPIRE].

[123] M. Cacciari, G.P. Salam and G. Soyez, *The anti-k_t jet clustering algorithm*, *JHEP* **04** (2008) 063 [arXiv:0802.1189] [INSPIRE].

[124] M. Cacciari, G.P. Salam and G. Soyez, *FastJet User Manual*, *Eur. Phys. J. C* **72** (2012) 1896 [arXiv:1111.6097] [INSPIRE].

[125] ATLAS collaboration, *Electron efficiency measurements with the ATLAS detector using the 2015 LHC proton-proton collision data*, ATLAS-CONF-2016-024 (2016).

[126] ATLAS collaboration, *Search for doubly charged Higgs boson production in multi-lepton final states with the ATLAS detector using proton–proton collisions at $\sqrt{s} = 13$ TeV*, *Eur. Phys. J. C* **78** (2018) 199 [arXiv:1710.09748] [INSPIRE].

[127] J.M. Campbell and R.K. Ellis, *An Update on vector boson pair production at hadron colliders*, *Phys. Rev. D* **60** (1999) 113006 [hep-ph/9905386] [INSPIRE].

[128] S. Catani and M. Grazzini, *An NNLO subtraction formalism in hadron collisions and its application to Higgs boson production at the LHC*, *Phys. Rev. Lett.* **98** (2007) 222002 [hep-ph/0703012] [INSPIRE].

[129] F. Campanario, V. Hankele, C. Oleari, S. Prestel and D. Zeppenfeld, *QCD corrections to charged triple vector boson production with leptonic decay*, *Phys. Rev. D* **78** (2008) 094012 [arXiv:0809.0790] [INSPIRE].

JHEP03(2022)195

[130] G. Balossini et al., *Combination of electroweak and QCD corrections to single W production at the Fermilab Tevatron and the CERN LHC*, *JHEP* **01** (2010) 013 [arXiv:0907.0276] [INSPIRE].

[131] A. Bredenstein, A. Denner, S. Dittmaier and S. Pozzorini, *NLO QCD corrections to* $pp \to t\bar{t}b\bar{b} + X$ *at the LHC*, *Phys. Rev. Lett.* **103** (2009) 012002 [arXiv:0905.0110] [INSPIRE].

[132] S. Catani, L. Cieri, G. Ferrera, D. de Florian and M. Grazzini, *Vector boson production at hadron colliders: a fully exclusive QCD calculation at NNLO*, *Phys. Rev. Lett.* **103** (2009) 082001 [arXiv:0903.2120] [INSPIRE].

[133] J.M. Campbell, R.K. Ellis and C. Williams, *Vector boson pair production at the LHC*, *JHEP* **07** (2011) 018 [arXiv:1105.0020] [INSPIRE].

[134] G. Bevilacqua and M. Worek, *Constraining BSM Physics at the LHC: Four top final states with NLO accuracy in perturbative QCD*, *JHEP* **07** (2012) 111 [arXiv:1206.3064] [INSPIRE].

[135] M.V. Garzelli, A. Kardos, C.G. Papadopoulos and Z. Trócsányi, $t\bar{t}W^{+-}$ *and* $t\bar{t}Z$ *Hadroproduction at NLO accuracy in QCD with Parton Shower and Hadronization effects*, *JHEP* **11** (2012) 056 [arXiv:1208.2665] [INSPIRE].

[136] D.T. Nhung, L.D. Ninh and M.M. Weber, *NLO corrections to WWZ production at the LHC*, *JHEP* **12** (2013) 096 [arXiv:1307.7403] [INSPIRE].

[137] N. Kidonakis, *Theoretical results for electroweak-boson and single-top production*, *PoS* **DIS2015** (2015) 170 [arXiv:1506.04072] [INSPIRE].

[138] C. Muselli, M. Bonvini, S. Forte, S. Marzani and G. Ridolfi, *Top Quark Pair Production beyond NNLO*, *JHEP* **08** (2015) 076 [arXiv:1505.02006] [INSPIRE].

[139] Y.-B. Shen, R.-Y. Zhang, W.-G. Ma, X.-Z. Li, Y. Zhang and L. Guo, *NLO QCD + NLO EW corrections to* WZZ *productions with leptonic decays at the LHC*, *JHEP* **10** (2015) 186 [*Erratum ibid.* **10** (2016) 156] [arXiv:1507.03693] [INSPIRE].

JHEP03(2022)195